Published in final edited form as:
J Comp Neurol. 2006 May 1; 496(1): 97–120. doi:10.1002/cne.20935.

The Chicken Suprachiasmatic Nuclei: I. Efferent and Afferent Connections

Elizabeth L. Cantwell and **Vincent M. Cassone**
Department of Biology and Center for Research on Biological Clocks, Texas A&M University, College Station, Texas 77843

Abstract

The avian circadian system is composed of multiple inputs, oscillators and outputs. Among its oscillators are the pineal gland, retinae and a hypothalamic structure assumed to be homologous to the mammalian suprachiasmatic nucleus (SCN). Two structures have been suggested as this homolog—the medial SCN (mSCN) and the visual SCN (vSCN). The present study employed biotin dextran amine (BDA) and cholera toxin B subunit (CTB) as anterograde and retrograde tracers to investigate the connectivity of the mSCN and vSCN in order to address this issue. Intravitreal injections of CTB were used to determine whether one or both of these structures receives afferent input from retinal ganglion cells. Both the vSCN and mSCN receive terminal retinal input, with the strongest input terminating in the vSCN. Precise iontophoretic injections of BDA and CTB in the mSCN and vSCN were used to identify efferents and afferents. The avian mSCN and vSCN collectively express more efferents and afferents than does the mammalian SCN. A subset of these connections matches the connections that have been established in rodent species. Individually, both the mSCN and vSCN are similar to the mammalian SCN in terms of their connections. Based on these data and other studies, we present a working model of the avian SCN that includes both the mSCN and vSCN as hypothalamic oscillators. We contend that both structures are involved in a suprachiasmatic complex that, as a functional group, may be homologous to the mammalian SCN.

Keywords

avian; CTB; BDA; tract tracing; retinohypothalamic; iontophoretic injection

INTRODUCTION

Circadian systems are composed of multiple inputs, oscillators and outputs. Timing cues are transmitted via input pathways to oscillators, which then drive rhythms and/or entrain sub-oscillators through output pathways (Menaker and Tosini, 1995). In vertebrates, these components comprise at least the retinae, the suprachiasmatic nuclei of the hypothalamus and the pineal gland, each of which vary in system-level importance among taxa and within each taxon (Menaker and Tosini, 1995).

In the mammalian circadian system, the suprachiasmatic nucleus (SCN) is the primary circadian pacemaker (Moore, 1979). First, the SCN receives significant direct retinal input via the retinohypothalamic tract (RHT) (Moore et al., 1971; Moore and Lenn, 1972; Moore, 1973). The SCN of eutherian mammals (but not of marsupial mammals) may be subdivided,

Corresponding author: Vincent M. Cassone, Professor and Head, Department of Biology, Texas A&M University, College Station, TX 77843-3258, phone: (979) 845-2301, fax: (979) 845-2891, email: vmc@mail.bio.tamu.edu.
Associate Editor: Paul Sawchenko

based on neuroanatomical and functional characteristics (Cassone et al., 1988b), into the retinorecipient ventrolateral SCN, known as the “core”, and the dorsomedial region, the “shell” (Moore et al., 2002). Secondly, surgical destruction of the entire SCN results in arrhythmic locomotor behavior (Moore and Eichler, 1972; Stephan and Zucker, 1972; Moore and Klein, 1974; Klein and Moore, 1979), and transplantation of fetal SCN tissue into the third ventricle of arrhythmic, SCN-lesioned rodents restores rhythmicity in locomotor activity (Drucker-Colin et al., 1984; Sawaki et al., 1984; Lehman et al., 1987). Finally, many aspects of SCN physiology oscillate with a circadian period, including glucose utilization *in vivo* and *in vitro* (Schwartz and Gainer, 1977; Schwartz et al., 1980; Newman et al., 1992), neuronal firing *in vivo* and *in vitro* (Inouye and Kawamura, 1979; Green and Gillette, 1982; Groos and Hendriks, 1982; Shibata et al, 1982), and gene expression *in vivo* and *in vitro* (Yamazaki et al., 2000; Hastings and Herzog, 2004).

Birds have a more complex circadian system than do mammals, since the pineal gland and retinae participate as independent oscillators and pacemakers as well. The pineal gland rhythmically synthesizes and secretes the hormone melatonin such that levels are high during the night and low during the day *in vivo* and *in vitro*, a rhythm that persists for up to four circadian cycles in constant darkness (DD; cf. Natesan et al., 2002). The retinae also rhythmically synthesize melatonin in chickens (Binkley et al. 1979, Hamm and Menaker 1980), Japanese quail (Underwood and Siopes 1984) and pigeons (Oshima et al., 1989; Adachi et al., 1995). This rhythm is important for overt circadian organization in some species. Bilateral enucleation results in the loss of rhythmic activity and body temperature in Japanese quail (Underwood and Siopes, 1984) and chickens (Nyce and Binkley, 1977). In pigeons, enucleation partially disrupts activity and body temperature rhythms but, when paired with pinealectomy, abolishes these rhythms (Ebihara et al., 1984; Chabot and Menaker, 1994).

Several features of circadian organization in birds suggest the presence of another oscillator in the anterior hypothalamus, possibly homologous to the mammalian SCN (Ebihara and Kawamura, 1981; Simpson and Follett, 1981; Takahashi and Menaker, 1982). Early cytoarchitectural evidence suggested that a region located near the preoptic recess of the third ventricle is the avian SCN (Crosby and Showers, 1969). This structure has been labeled the periventricular preoptic nucleus (PPN; van Tienhoven and Jühász, 1962; Cassone and Moore, 1987; revised nomenclature, POP; Kuenzel and Masson, 1988), the SCN (Hartwig, 1974, Kuenzel and van Tienhoven, 1982; Brandstatter et al., 2001), the medial hypothalamic nucleus (MHN; Norgren and Silver, 1989), the medial hypothalamic retinorecipient nucleus (MHRN; Shimizu et al., 1994) and the medial SCN (mSCN; Kuenzel and Masson, 1988; Yoshimura et al., 2001). In the present study, we will refer to this structure as the mSCN. The mSCN has been reported to receive some retinal afferents, but the label is typically weak (Hartwig, 1974; Oliver et al. 1978) or undocumented with photomicrographs (Ebihara and Kawamura, 1981).

In contrast, a lateral hypothalamic nucleus is the primary, if not only, hypothalamic retinorecipient nucleus in a variety of species: ringed turtledove, *Streptopelia risoria* (Cooper et al., 1983; Norgren and Silver, 1989), house sparrow, *Passer domesticus* (Cassone and Moore, 1987), pigeon, *Columba livia* (Meier, 1973; Gamlin et al., 1982; Shimizu et al., 1994), duck, *Anas platyrhynchos* (Bons, 1976) and chicken, *Gallus domesticus* (Shimizu et al., 1984). This structure has been referred to in the literature as the SCN (Gamlin et al, 1982; Cooper et al., 1983), the lateral hypothalamic retinorecipient nucleus (LHRN; Norgren and Silver, 1989; Shimizu et al., 1994) and the visual SCN (vSCN; Cassone and Moore, 1987). In this study, we will use the term vSCN.

Antigen mapping has also been utilized to identify the avian SCN. The SCN of mammals is heterogeneous in its antigen distribution. In rodents, cells immunoreactive for vasoactive intestinal polypeptide (VIP) are found in the core, while arginine vasopressin (AVP) immunoreactive cells are found in the shell (Moore et al., 2002). Similarly, in the house sparrow, AVP (avian homolog, arginine vasotocin) immunoreactive cells are found ventral to the vSCN, while VIP positive cells are found at the medial border of the vSCN (Cassone and Moore, 1987). Other antigens found in the mammalian SCN include gastrin releasing peptide, glutamic acid decarboxylase, neuropeptide Y, neurotensin, serotonin, somatostatin and substance P (Moore et al., 2002), all of which are found in the vSCN of the house sparrow (Cassone and Moore, 1987). While the chemoarchitecture of the vSCN is similar to that of the eutherian mammalian SCN, it is not identical; therefore, it was proposed by Cassone and Moore (1987) that the vSCN is the retinorecipient portion of a suprachiasmatic complex in which one or more other structures may be involved.

The present study is an analysis of the synaptic connections of both the vSCN and the mSCN of the chicken, *Gallus domesticus*, and examines whether efferent and afferent connections of and between the mSCN and vSCN indicates whether one or both may be homologous to the mammalian SCN. We present here a new working model of the avian SCN based on the current and previous studies.

MATERIALS AND METHODS

Animals

Female Spangled Old English Bantams (*Gallus domesticus*) were acquired at Ideal Poultry (Cameron, TX) on their hatch date. Male White Leghorn chicks (*Gallus domesticus*) were obtained, also on their hatch date, from Hy-Line Hatcheries (Bryan, TX). Birds were housed on a light:dark 12:12 cycle (lights on from 6:00 a.m. to 6:00 p.m. CST) until the injections took place. Both strains were raised in heated brooders: the White Leghorns remained in the brooders, while the Bantams were moved to unheated cages and grown to adulthood, about two to three months, to achieve a stable weight (450–720 g) before surgery. Injections were performed on White Leghorns once their weight reached 275–310 g, which took four to five weeks. Food (Purina Start and Grow; Brazos Feed & Supply, Bryan, Texas) and water were continuously available until the day of the surgery, at which time they were removed. All animal use protocols were reviewed and approved by the University Laboratory Animal Care Committee (ULACC) at Texas A&M University (Animal Use Protocol #2001–163).

Determination of stereotaxic coordinates

Stereotaxic coordinates for the vSCN and mSCN were determined using 26 White Leghorn chicks. Chicks were deeply anesthetized with ketamine/xylazine drug cocktail (90 mg/kg ketamine, 10 mg/kg xylazine) and placed into a stereotaxic apparatus equipped with ear and beak bars specialized for birds. In order to ensure a stable angle, coordinates were taken from three points: ear bar zero was used as the reference point, eye corner zero represented the coordinates of the posterior corner of the eye and lambda designated the coordinates at the intersection of the lambdoid and sagittal sutures of the cranium. A stable slope was established and test lesions were performed. After each lesion, the birds were immediately sacrificed; their brains were removed and flash frozen. Brains were sectioned frontally at 30 μm, thaw-mounted onto slides, fixed in alcohol, stained with cresyl violet, dehydrated, cleared and coverslipped for localization of the lesions. After obtaining a rough location for the mSCN and vSCN, the coordinates were refined such that we could reliably target these structures with the thin micropipettes used for intracerebral iontophoresis.

Tract tracing agents

Cholera Toxin B-subunit (CTB) is a sensitive tracing agent widely used in anatomical studies. It functions as an anterograde (Wu et al., 1999) and retrograde (Calaza and Gardino, 2000) tracer when injected intravitreally. Injected intracerebrally, CTB also traces anterogradely and retrogradely. There is some evidence that suggests CTB is avidly taken up by fibers of passage (Chen and Aston-Jones 1995); therefore, it is more useful as a retrograde tracer. CTB has been used extensively in mammalian mapping studies, and many studies have demonstrated comparable efficacy in birds (Shimizu et al., 1994; Wu et al., 2003; Gardino et al., 2004). We also used 10,000 kD biotin dextran amine (BDA) as an anterograde tracing agent. Previous studies have shown its ability to label both axons and terminals in efferent structures in birds (Veenman et al., 1992; Tombol et al., 2003). Neither CTB nor BDA cross synapses over short incubation periods, thus, labeling identifies direct afferents or efferents to injected and iontophoresed sites.

Intravitreal injection of CTB

Five birds were anesthetized with ketamine/xylazine drug cocktail. The eyelid was deflected and 20 μl 0.5% CTB (List Biological Laboratories, Campbell, CA) was injected into the vitreous chamber of the eye with a 50 μl Hamilton syringe. The syringe was left in place for two minutes while the CTB diffused away from the tip, at which time it was removed. These birds were maintained in a separate cage for two (n=4) or five (n=1) days until they were sacrificed. At a later date, two additional birds were anesthetized and injected intravitreally with 20 μl of Alexa Fluor 594 (Texas-Red)-conjugated CTB (1 mg/ml; Molecular Probes, Eugene OR) in the manner described above. They were sacrificed after five days survival.

Iontophoretic CTB injections

The first set of CTB iontophoretic injections was performed in the Bantam chickens. Glass micropipettes (tip diameter 5–10 μm) were backfilled with 1% CTB solution after which 5 μl were loaded into each micropipette using a 10 μl Hamilton syringe. Twenty-six Bantams were anesthetized with ketamine/xylazine drug cocktail and the proper head angle in a stereotaxic apparatus was achieved as described above. The micropipette was slowly lowered to the proper coordinates and allowed to settle for ten minutes. A 5 μA current was then applied to the CTB solution for a five-minute cycle of 7 seconds on/7 seconds off using a Midgard power supply (Stoelting Co., Wood Dale, IL). In Bantams, we directed twelve unilateral injections at the vSCN and fourteen at the mSCN. Upon completion of iontophoresis, the micropipette was left in place and the CTB solution was allowed to diffuse away from the tip of the electrode for at least ten minutes, at which time the micropipette was removed from the brain and the scalp was stitched closed.

White Leghorns (n=13) were injected in a second round of similar surgeries after the Bantam brains were processed and visualized. Micropipettes were loaded, as described above, but this time with 0.5% CTB. Eight injections were directed at the vSCN, five at the mSCN. A 5 μA current, alternating on and off for 7 seconds, was applied to the CTB solution for ten minutes. After ten minutes of diffusion time, the micropipette was removed while the CTB solution was under a continuous -5 μA current to further ensure that none leaked into the track made by the micropipette. These animals were maintained for five days.

Iontophoretic BDA injections

Glass micropipettes (tip diameter 20–30 μm) were backfilled with 10% BDA (Molecular Probes, Eugene, OR) in 0.01 M phosphate buffer after which 5 μl were loaded into each micropipette using a 10 μl Hamilton syringe. White Leghorn chicks (n=23) were

anesthetized with ketamine/xylazine drug cocktail and the surgical insertion of the micropipettes was performed as described above. A +5 μA current was applied to the BDA solution for twenty minutes in 7-second on/off cycles. Twelve injections were directed at the vSCN, eleven were aimed at the mSCN. After iontophoresis, the micropipette was left in place and the BDA solution was allowed to diffuse away from the tip of the electrode for at least ten minutes. The micropipette was removed from the brain under constant negative current and the scalp was stitched closed. These animals were maintained for eight days.

Tissue preparation

Birds were anesthetized with ketamine/xylazine drug cocktail, which was supplemented as needed with halothane. White Leghorn eyes were removed prior to fixation and the retinae were removed and fixed in 4% paraformaldehyde. Birds were transcardially perfused with 50–100 ml phosphate buffered saline (PBS; 10mM, pH 7.4), followed by 300–500 ml 4% paraformaldehyde fixative. Brains were subsequently removed and post-fixed for 4–16 hours. They were then cryoprotected in serial solutions of 10%, 20% and 30% sucrose.

Brain tissue processing

Cryoprotected brains were frozen, frontally sectioned at 30 μm on a Lipshaw cryostat (Pittsburgh, PA). Slices were collected in four bins of adjacent sections. One bin, comprising sections spaced 120μm apart, were rinsed in PBS. Endogenous peroxidase activity was inhibited with a 15-minute incubation of 30% methanol and 0.75% hydrogen peroxide in PBS followed by a blocking step in PBS containing 0.3% Triton-X-100 and 1% normal rabbit serum (PBSRT) for 1 hour. All sections processed for CTB immunoreactivity were incubated with goat anti-choleragenoid antibody (1:5000; List Biological Laboratories, Campbell, CA) in PBSRT for 48–72 hours at 4°C, followed by biotinylated rabbit anti-goat secondary antibody (1:200; Vector Laboratories, Burlingame, CA) in PBSRT for two hours at room temperature. Sections were incubated with avidin-biotin complex from a peroxidase standard kit (1:55; Vector Laboratories, Burlingame, CA) in PBSRT, in the case of CTB, or PBS containing 0.4% Triton-X-100, in the case of BDA, for 90 minutes at room temperature. Sections were incubated in 0.5% 3-3′-diaminobenzidine solution in 100 mM Tris buffer for five minutes after which 0.21% hydrogen peroxide was added to the solution. The color reaction was stopped as soon as background coloration became evident. Sections were rinsed, put into order, mounted onto gelatin-coated slides and dried overnight. The slides were then rinsed in PBS and the color reaction was stabilized in 1% cobalt chloride solution. The slides were rinsed, dehydrated, cleared and coverslipped for analysis.

Retinal processing

Intact retinae were processed for visualization of BDA and CTB in the manner described above. After the color reaction, the retinae were float mounted onto slides. They were then processed and coverslipped in the same manner as the brain sections.

Microscopy and photography

An Olympus BH-2 light microscope (Melville, NY) was used to examine processed tissues. CTB immunoreactivity was observed with differential interference contrast optics, while BDA immunoreactivity was viewed under dark field. Photomicrographs were taken with an Olympus C-35AD-4 camera on Kodak Gold 200 film (Rochester, NY). Prints were scanned at 600 DPI and opened in Adobe Photoshop 7.0.1 (Adobe Systems, Mountain View, CA), where they received minor brightness and contrast adjustments.

Evaluation of injection sites and tracing

CTB and BDA injection sites appeared similar to one another and were readily identified by dense immunoreactive fields surrounding central necrotic areas. Previous studies have demonstrated that CTB and BDA are taken up and transported from the most densely labeled region (Leak and Moore, 2001). Photomicrographs of reported injection sites are available in Figure 1. Injection sites outside the border of these structures were used for two purposes. First, Bantam and White Leghorn afferents and efferents were compared in brains that had similar injection sites. In this way, we were able to determine that there are no significant differences between the connections of the vSCN and mSCN of these two strains. Secondly, injections that missed the SCN entirely were used to assess the accuracy of our maps. In the analysis of tract tracing, we also took into account whether BDA labeled fibers were terminal or fibers of passage. Terminal fibers were identified by the presence of varicosities and fibers of passage by their thick, smooth appearance.

Mapping

CTB cells and fibers and BDA fibers were drawn free hand and then digitized onto plates adapted from a published chick stereotaxic atlas (Kuenzel and Masson, 1988). Brain structures were identified according to the nomenclature of Kuenzel and Masson (1988) and several published partial atlases (Kuenzel and van Tienhoven, 1982; Ehrlich and Mark, 1984; Reiner et al., 2004).

In order to produce a map of the retina, a slide was placed on a light box and the outline was drawn onto a transparency. The traced image was put onto an overhead projector for enlargement. The enlarged image was scanned into Photoshop where the distribution of retinal ganglion cells was digitally recorded.

RESULTS

Retinal projections

Three intravitreal injections that transported for two days before sacrifice resulted in strong labeling of retinal terminals in the chick brain. Two brains were strongly labeled after five days of transport: one resulted from injection of unconjugated CTB, while the other was a product of Alexa Fluor 594-conjugated CTB injection. There were no significant differences between the label that resulted from the injection of these two different tracers. Sections from these brains were used to produce maps (Fig. 2) and photomicrographs (Fig. 3). We observed retinal terminals and, in the case of the isthmo-optic nucleus, cells, in many structures previously identified by tract-tracing methods and retinal degeneration. A summary of these structures is provided in Table 1. Of particular interest in this study was a terminal field in the vSCN (Fig. 2C–E). This region was more strongly labeled after five days of transport (Fig. 3E) than it was after two days (Fig. 3F). Labeled sparse cells were also identified within vSCN, and were more easily identified after two days of CTB transport (Fig. 3F inset) than they were after five days. Sparse label in the lateral mSCN indicated both terminal fibers and fibers of passage (Figs. 2A, 3C). Staining in several other structures identified has not been previously reported. Retinal terminals were also observed in the region dorsal to the mSCN, including the ventral aspect of the hypothalamic anterior nucleus (AM) and the region between mSCN and AM (Fig. 3C). We also found terminal fibers in a contralateral region of the anterior diencephalon that we believe may be homologous to the mammalian ventrolateral preoptic nucleus (VLPO). Modest staining in the form of discernible terminal fibers was observed in this structure roughly 500 μm anterior to the vSCN and 750 μm lateral of the mSCN, which was in the same frontal planes of section (Figs. 2A, 3A,C). Finally, terminals were found in the ipsilateral nucleus triangularis (T; Fig. 3I), dorsolateral anterior nucleus, rostrolateral part (DLAlr; Fig. 3J) and

the lateral anterior nucleus (LA; Fig. 3J). All of these structures also receive strong contralateral input.

Iontophoretic injections

Two BDA injections were identified within the medial suprachiasmatic nucleus (mSCN). One was isolated to the mSCN with minor leakage caudally (Fig. 1A), while the second impinged upon the optic chiasm with some possible leakage into the third ventricle (Fig. 1B). Projections that were identified in both mSCN-injected brains are reported in Table 2. Projections present in one brain and not the other are not described. Of the nine remaining injections, two were discarded due to poor tracer administration. Four injections were completely misplaced, resulting in projection patterns bearing no similarity to the mSCN efferents observed. They are not reported. The final three injections were analyzed in order to critically evaluate our potential mSCN efferents. The first injection was located in the mSCN, but extended dorsally to the ventral aspect of AM (Fig. 1C). The second injection was localized specifically to AM (Fig. 1D), while the third was also located in AM, but extended rostrally into the preoptic area (POA; Fig. 1E). The efferents identified as a result of these injections are noted in Table 2.

Two CTB injections were identified within the borders of the mSCN. The first extended laterally into the preoptic area and ventrally into the optic chiasm (CO) with a small amount of leakage into the third ventricle (Fig. 1F). The second was relatively well-contained, with only a small amount of leakage into the third ventricle (Fig. 1G). The resulting afferent projections to the mSCN are listed in Table 3. Of the seventeen remaining injections, five were discarded due to large scale leakage of tracer into the pipette track, two were discarded because tracer delivery was not apparent, likely due to a clogged micropipette tip, and one was discarded because the micropipette was deflected to a distal region, the afferents of which are significantly different than those resulting from the mSCN injections. The final eight injections were sorted into three groups—one very large injection encompassing most of AM and the dorsal aspect of mSCN (Fig. 1H), three injections to POA with impingement on CO (Fig. 1I) and four injections that delivered tracer to the third ventricle (3V; Fig. 1J) were used to evaluate our reported mSCN afferents and are included in Table 3. One injection to CO was analyzed and it was found that no cellular staining resulted; therefore, we did not include this injection in Table 3.

Three BDA injections were limited to the borders of the vSCN (Fig. 1K–M). One of these injections was situated dorsally compared to the other two (Fig. 1L) and one impinged slightly on DSV (Fig. 1M), but there were no significant differences in their efferent projections, which are reported in Table 2. Of the remaining nine injections, two were discarded due to lack of tracer delivery, while four injections were misplaced into either white matter tracts or distal areas bearing no efferent projection similarity to the three vSCN injections. Three injections were of particular interest and were used in our assessment of vSCN efferents. The first injection was located in the optic tract (TrO; Fig. 1N), while the other two were situated atop the vSCN dorsal border, one in the ventral supraoptic decussation (DSV; Fig. 1O) and the other into gray matter dorsal and slightly lateral to vSCN, between GLv and DSV (Fig. 1P).

Three CTB injections were identified within the borders of the vSCN. One of these injections was very well confined within the nuclear border (Fig. 1Q). The other two injections overflowed the border slightly into adjacent gray matter (Fig. 1R–S). No significant differences were evident in their afferents, which are reported in Table 3. Of the seventeen remaining injections, three were discarded due to tracer leakage into the track or deficient tracer delivery and four were discarded as the injection location was distal and the resulting afferent projections were significantly different than those found with vSCN

injection. The remaining injections were grouped into four categories. One large injection included the dorsal vSCN, the gray matter dorsal to vSCN and four fiber tracts (white matter; WM): the dorsal supraoptic decussation (DSD), DSV, the medial forebrain bundle and the quinto-frontal tract (Fig. 1T). A second injection was located further dorsal in the intercalated nucleus (ICT; Fig. 1U). Two CTB injection sites encompassed the vSCN and impinged upon the medial aspect of GLv (Fig. 1V). Four injections were located within GLv (Fig. 1W), two of which extended slightly into the ventrolateral thalamic nucleus (VLT). The final two injections were located within TrO. No afferent cells were identified as a result of the TrO injections and they are therefore not included with the reported injections of interest in Table 3.

Most labeling from both BDA and CTB iontophoretic injections was ipsilateral. Therefore, unless specifically identified as contralateral, all structures described are ipsilateral to the injection site.

Efferent connections

The mSCN and vSCN efferents in which terminal fibers were identified are summarized in Table 2. Maps of mSCN efferents are shown in the right hemispheres of the left-hand panels of Figure 4, and representative photomicrographs are compiled in Figure 5. Efferents from the vSCN are mapped in Figure 6 left panels and representative photomicrographs are shown in Figure 7.

We found mSCN efferent terminal fibers primarily in structures along the midline of the chick brain. Fibers terminate in the lateral septal nucleus (SL; Fig. 4A–E) and the bed nucleus of the stria terminalis (nBST; Fig. 4A–E) of the telencephalon. In the diencephalon, terminal fibers are found in the preoptic area (POA), including the medial preoptic nucleus (POM; Fig. 4A), preoptic periventricular nucleus (POP; Fig. 4B), dorsolateral preoptic nucleus (POD; Fig. 4A) and ventral supraoptic nucleus (SOv; Fig. 4A). Hypothalamic efferents include AM (Figs. 4B–F, 5K), the lateral hypothalamic area (LHy; Figs. 4E–L; 5K) and the ventromedial nucleus (VMN; Fig. 4G–K). The contralateral mSCN receives input, as does the ipsilateral (Figs. 4F,G, 5O,P) and contralateral (Fig. 5N) visual suprachiasmatic nucleus (vSCN). In the tuberal hypothalamus, efferent fibers terminate in the hypothalamic inferior nucleus (IH) (Figs. 4L–N, 5M), the infundibular nucleus (IN; Figs. 4L–N, 5M), dorsomedial nucleus (DMN; Fig. 4L) and the medial mammillary nucleus (MM; Fig. 4O). Finally, strong signal is present in the hypothalamic paraventricular nucleus (PVN; Fig. 4D–I), from which fibers of passage oriented toward the thalamic paraventricular nucleus (PVT; Figs. 4D–K, 5L) originate. PVT is labeled and fibers of passage in the dorsal portion of PVT are directed toward nBST of the telencephalon. The habenular region is stained with terminal fibers (Figs. 4G–M, 5J). A few structures associated with the visual system are labeled, including the perirotundal area (pRot; Fig. 4H–K) and the pretectal area (AP; Fig. 4N). The periventricular gray layer (SGP; Fig. 4N–T) and the central album layer (SAC; Fig. 4N–P) of the optic tectum contain labeled fibers. Finally, terminal fibers are located in the bed nucleus of the pallial commissure (nCPa; Fig. 4B–D) and the central gray (GCt; Fig. 4N–Q).

Efferent projections identified by the mSCN/AM injection included all of the efferents identified by mSCN injection alone. Many of these projections were more abundant from this more dorsal injection site, particularly efferents to SL, nBST and the habenula. In addition to these projections, mSCN/AM injection identified efferents in several thalamic structures as well as the ventral tegmental area (AVT). These additional efferents were also identified by AM injection alone and by the AM/POA injection.

Efferents from the vSCN are generally found more laterally in the chick brain. In POA of the diencephalon, terminals are found in SOv and POM (Fig. 6A). Many structures receiving efferents from the vSCN are in the hypothalamus, including AM (Fig. 6B–E), anterior LHy (Fig. 6E), mSCN (Figs. 6B,C, 7J), VLPO (Figs. 6B,C, 7N), ansa lenticularis (AL; Fig. 6F–J) and the contralateral vSCN. Fibers of passage in DSD and the ventral supraoptic decussation (DSV; Fig. 6F–I) are apparent. Many structures associated with visual function receive efferents of the vSCN. In the thalamus, VLT (Figs. 6B–E, 7K), LA (Figs. 6B–E, 7K), the dorsal border of GLv (Fig. 6E–L), the intercalated nucleus (ICT; Fig. 6F,G), dorsolateral anterior nucleus magnocellular part (DLAmc; Fig. 6E), lateral part (DLAl; Fig. 6F–H), medial part (DLAm; Fig. 4F–H) and rostrolateral part (DLAlr; Fig. 6E–G), the dorsolateral posterior nucleus (DLP; Fig. 6I) and the dorsal border of the dorsolateral geniculate nucleus (GLd; Fig. 6I–M), contain terminal fibers. In the pretectum, efferent terminals are in pRot (Fig. 6F–I), the subpretectal nucleus (SP; Fig. 6M,N), principal precommissural nucleus (PPC; Fig. 6H–K), pretectal nucleus (PT; Fig. 6M), AP (Figs. 6M, 7M), LMmc (Fig. 6H–K) and LMpc (Fig. 6I–K). In the mesencephalon, terminal fibers are found in the optic tectum (Fig. 6L–T)—SGP and SAC (Fig. 7L), the central gray layer (SGC) and superficial fiber and gray layer (SGFS) all contain terminal fields. SGP and SAC fibers are primarily ventral, although sparser staining is present dorsally. In the SGC and SGFS, fibers are localized only to the ventral portion of the optic tectum. Nucleus ovoidalis (OV; Fig. 6I), GCt (Fig. 6M–S), the nucleus of the basal optic root (nBOR, Fig. 6M–Q), the pedunculopontine tegmental nucleus (PPT; Fig. 6P,Q), AVT (Fig. 6Q), the red nucleus (Ru; Fig. 6O–Q) and the contralateral medial nucleus of Edinger-Westphal (EWm; Fig. 7I), as well as the papillioform nucleus (Pap; Fig. 6R–T) of the rhombencephalon receive efferent projections.

The misplaced injection to TrO labeled a limited subset of retinorecipient regions, as is delineated in Table 2. Two injections dorsal to vSCN were analyzed. Injection to DSV resulted in efferent projections that are similar to vSCN efferents, but are much less abundant. Injection to the gray matter just dorsal to the vSCN identified, again, a similar set of efferent projections that were generally less abundantly labeled, while strongly labeling the vSCN itself.

Afferent connections

Afferents of the mSCN and vSCN are summarized in Table 3. Maps of mSCN afferents are shown in the right-hand panels of Figure 4, and representative photomicrographs are displayed in Figure 5. Afferents of the vSCN are mapped in Figure 6 right panels and representative photomicrographs are shown in Figure 7.

Telencephalic afferents to the mSCN include the hippocampus (Hp; Figs. 4A, 5I), parahippocampal area (APH; Fig. 5H), nucleus taeniae (Tn; Figs. 4F–I, 5E), SL (Fig. 4A–E) and nBST (Fig. 4A–E). In the diencephalon, POA afferents include MPO, SOv and POD (Fig. 4A) and POP (Fig. 4B). In the hypothalamus, AM (Fig. 4B–F), PVN (Fig. 4D–L), the contralateral mSCN, VLPO (Figs. 4B,C, 5F), LHy (Fig. 4C–K), VMN (Figs. 4G–K, 5B) and the anterior vSCN (Figs. 4F, 5C) are also labeled. In the tuberal hypothalamus, IH (Figs. 4L–N, 5A), IN (Figs. 4L–N, 5A), DMN (Fig. 4L), MM (Figs. 4O, 5G) and the median eminence (ME; Figs. 4L–P, 5A) contain afferent cells. In the thalamus, cells are seen in LA (Fig. 4B–E), VLT (Fig. 4B–E), nCPa (Fig. 4B–D) and PVT (Figs. 4D–I, 5D). The habenular region is also afferent to the vSCN (Figs. 4G–L). In the mesencephalon, SGP (Fig. 4N,O) and SAC (Fig. 4O–S) of the optic tectum are labeled. Finally, afferent cells are found in GCt (Fig. 4N–T) and AVT (Fig. 4R).

A large, misplaced injection that encompassed AM and the dorsal portion of mSCN identified a set of afferents similar to that of mSCN. In some cases, afferents were more abundant after mSCN injection; in others they were more abundant after AM/mSCN

injection. This is different from the situation with efferents, where we found that mSCN/AM injection resulted in generally more abundant projections than mSCN only. Additional afferents identified after AM/mSCN injection presumably originate from AM itself; however, no injection to AM was limited within that nucleus only. POA/CO injection resulted in a limited subset of stained afferents, which are also afferent to mSCN, in addition to mSCN itself. In general, these afferents were less abundant from POA/CO. Delivery of the entire volume of CTB to the third ventricle labeled a set of cell bodies similar to the afferents that project to mSCN; however, the appearance of this staining was markedly different from cellular stain resulting from CTB injection to the mSCN. In the case of transport from the mSCN, labeled fibers associated with the projecting cell bodies were oriented dorsoventrally and were relatively light in their appearance. In contrast, cell bodies stained by uptake of CTB from the third ventricle were more closely associated with the cavity than were those labeled by transport from mSCN injections. Further, the processes associated with these cells were very dark and were oriented mediolaterally, extending from the ependymal border of the third ventricle to the closely apposed cell bodies. Staining of cell bodies in more distal regions such as Hp, nBSTL, SL an the visual Wulst (HA) is presumably a result of transport of CTB within the cerebrospinal fluid, which contacts all structures identified.

Telencephalic structures afferent to the vSCN include HA (Figs. 6A, 7B) and APH (Fig. 7A). The hypothalamic AM (Fig. 6B–E), rostral LHy (Fig. 6E–H), mSCN (Figs. 6B,C, 7H), rostral and caudal, but not middle PVN (Figs. 6D,E,J–N, 7D) and VMN (Fig. 6F–J) contain afferent cells. Label is also found in VLPO (Fig. 6C,D), AL (Fig. 6F–K), contralateral vSCN (Fig. 7F) and IH (Fig. 6K,L). Afferents in the thalamus include LA (Fig. 6C–E), the dorsal border of GLv (Fig. 6E–L), nCPa (Fig. 6B–D), VLT (Fig. 6D,E), ICT (Fig. 6F,G), PVT (Fig. 6E–H), DLAmc (Fig. 6E), DLAl (Fig. 6F–H), DLAm (Fig. 6F–H), GLd (Fig. 6I–M) and T (Fig. 6H,I). In the pretectum, afferent cells are found in pRot (Figs. 6G–J, 7E), PPC (Figs. 6H–K, 7E), PD (Fig. 6L), PT (Fig. 6M), AP (Fig. 6M), LMmc (Figs. 6H–K, 7E) and LMpc (Figs. 6I–K, 7E). In the mesencephalon, all four layers of the optic tectum are afferent (Fig. 6L–T). Cells are denser in the ventral region of the tectum, with sparser staining in the dorsal regions. SGFS cells are found only it its ventral aspect. Afferent cells are found in the tectal gray (GT; Figs. 6L,M, 7G), GCt (Figs. 6M–S, 7C), locus coeruleus (LoC; Fig. 6S), the external cellular layer (SCE; Fig. 6L–N), nBOR (Fig. 6M–Q), Pap (Fig. 6R–T) and the oculomotor tract (OM; Fig 6N).

The misplaced injection to the dorsal vSCN/WM resulted in labeling of a very similar set of afferents as the vSCN injection itself, and they were either of comparable abundance or were less abundant. Injection to ICT labeled a much more limited set of afferents, all of which we identified as vSCN afferents, and are, in general, less abundant than those of the vSCN. Afferents labeled from the medial GLv and lateral vSCN are also similar, but less abundant, than vSCN afferents. Finally, very few afferents were identified after injection to the medial GLv.

The retinae from CTB-injected birds were examined for retinal ganglion cells (RGCs). Afferent RGCs were identified in the retinae contralateral to the vSCN injections and were used to create a distribution map (Fig. 8A) and photomicrographs of representative RGCs (Fig. 8B). RGCs are located throughout the dorsal portion of the retina. The distribution appears as a dense band with a sparse region of cells surrounding it. The cells are more dense centrally and less dense around the periphery of the dorsal retina. The cells are smaller toward the central region of the distribution, with slightly larger cells in the periphery. No RGCs were found in the retinae of mSCN- or mSCN/AM-injected birds.

DISCUSSION

Similarities to the mammalian SCN exist within both the mSCN and the vSCN. Data from the work presented here and previous studies, taken as a whole, indicate that both the mSCN and vSCN are involved in the avian circadian system. We propose below a new working model of the avian suprachiasmatic nucleus based on these observations.

Retinal projections

The data presented here indicate that the vSCN receives completely contralateral retinohypothalamic input. Following iontophoretic injections of CTB to the vSCN, numerous RGCs are labeled in the contralateral retina only. The finding that this retinal input derives from RGCs in the dorsal retina differs significantly from what has been found in the hamster, which sends a retinohypothalamic projection from RGCs that are distributed evenly throughout the retina (Pickard, 1982). The dorsal distribution of retinohypothalamic RGCs in chick, however, may be expected, since the dorsal region of the chick retina contains a denser population of RGCs than does the ventral aspect (Chen and Naito, 1999). As has been reported previously (see Table 1), sparse retinal input to the mSCN was also observed; however, the paucity of labeled terminal fibers in this structure and the absence of CTB-labeled RGCs in the retinae of mSCN-injected birds indicate that the vSCN is the primary retinorecipient structure in the chick hypothalamus. It is natural, given the melanopsin data obtained in current years (Gooley et al., 2003), to wonder whether it is also present in RGCs that project to either avian SCN. This is likely the case, as melanopsin mRNA (Bailey and Cassone, 2005) and protein (Chaurasia et al., 2005) expression has been demonstrated in all layers of the chick retina, including the retinal ganglion cell layer.

Interestingly, a classical study, employing autoradiographic techniques, reported abundant retinopetal cells present throughout the suprachiasmatic region of the pigeon and the jackdaw, *Corvus monedula*, including both the vSCN and the mSCN (Meier, 1973). In our study, cells were retrogradely labeled in the vSCN alone. These cells were clearly visible after two days of CTB transport but were generally obscured by the retinal terminal field after five days of transport. We attempted to confirm an efferent from the vSCN to the retina by viewing retinae from chicks in which BDA was injected into the vSCN but, because of the pigmentation in the retina, background was too high under dark field microscopy to identify BDA immunoreactive fibers. The data suggest a putative modulatory role for the vSCN on the retina, which is worthy of further study.

Retinal terminals identified in other structures have been reported previously (Table 1). Because they are outside the scope of this study and have already been described, we will not discuss them. We did, however, identify a previously unreported contralateral retinal projection that is of particular interest. This structure is in the same frontal plane as, and is lateral to, the rostral mSCN. This region contains γ-aminobutyric acid (GABA) immunoreactive cells with fibers visible at the dorsal margin (unpublished data). The mammalian VLPO is retinorecipient (Lu et al., 1999) and one of its primary antigens is GABA (Sherin et al., 1998); therefore, we believe this structure may be homologous to the mammalian VLPO, which has been implicated in regulation of sleep: wake cycles in mammals (Lu et al. 1999).

Efferents of the suprachiasmatic nuclei

With the exception of one investigation into human hypothalamic efferents of the SCN (Dai et al., 1998), studies investigating efferent connectivity of the SCN have focused on three rodents—rat, hamster and mouse (Stephan et al., 1981; Watts and Swanson, 1987; Watts et al., 1987; Kalsbeek et al., 1993; Morin et al., 1994; Abrahamson and Moore, 2001; Leak and

Moore, 2001; Kriegsfeld et al., 2004). In a few of these studies, efferents from the core and the shell regions have been divided in order to compare the two subdivisions of the nucleus. This division of mammalian SCN efferents may be seen in Figure 9B. In the present study, mSCN and vSCN projections are predominantly ipsilateral, as is the case in all mammals studied, and they are summarized in Figure 9A.

The mSCN and the rodent SCN exhibit several common efferents. Of particular interest are the projections to SL and nBST: the mammalian SCN also sends efferents to nBST and SL of the basal forebrain. These efferents are interesting because they are closely apposed to the lateral septal organ (LSO) in the chick. Previous studies have suggested that encephalic photoreceptors are located in LSO (Vigh-Teichmann et al., 1980; Silver et al., 1988; Kuenzel, 1993; Li et al., 2004; Rathinam and Kuenzel, 2005). The current data indicate a possible means of interaction between the mSCN and these putative encephalic photoreceptors. The vSCN makes fewer connections that are comparable to rodent SCN efferents. Most notable is a connection to VLPO, which receives projections from the SCN in the hamster (Kriegsfeld et al., 2004) and the rat (Chou et al., 2002). Several mammalian SCN efferents are comparable to structures efferent from both the mSCN and vSCN in the chick, as is delineated in Table 2.

The present data indicate that the total number of structures efferent from the mSCN and vSCN combined exceeds the number of known mammalian SCN efferents. One vSCN efferent reported here, contralateral EWm, has been well characterized in the pigeon (Gamlin et al., 1982). Because our BDA-labeled efferents were significantly more sparse than those previously identified, we referred to CTB-labeled fibers from vSCN injected birds and observed a more abundant efferent connection, presumably due to the larger CTB injection sites. EWm has been shown to regulate choroidal blood flow in the eye via parasympathetic circuits involving the ciliary ganglion (Fitzgerald et al., 1990; Reiner et al., 1990). A few efferent connections are made by the mSCN to tectofugal pathway structures; however, the vSCN exhibits a high degree of connectivity with visual structures of the tectofugal, thalamofugal and accessory optic pathways. In the chick, c-fos expression is induced in the vSCN by novel visual motion, supporting a role for the vSCN in the visual system (Wallman et al., 1994). Previous studies have indicated a role for the circadian system in the regulation of the visual system. In pigeons, parameters of both visually evoked potentials in the optic tectum and electroretinograms are rhythmic in both a 12:12 light:dark cycle (LD) and in constant darkness (DD; Wu et al., 2000). The distribution of vSCN efferents in the optic tectum, homologous to the mammalian superior colliculus, is particularly interesting because SGFS fibers are located only on its ventral aspect (Fig. 6). Electroretinogram parameters are also rhythmic in LD and DD in chicks (McGoogan and Cassone, 1999). Although the avian retina clearly contains the machinery for endogenous oscillation (Bailey et al., 2004), it is intriguing to speculate modulation of retinal function directly via vSCN efferents (Fig. 3E). The scope of efferent connectivity from the vSCN to visual system structures strongly supports the view that it is involved in circadian visual regulation in the retina, in retinorecipient structures and in integrative structures associated with visual processing. This view fortifies, perhaps coincidentally, the use of the term “visual suprachiasmatic nucleus”.

Afferents of the suprachiasmatic nuclei

Few studies have mapped the afferents of the mammalian SCN (Pickard, 1982; Morin at al, 1994; Moga and Moore, 1997; Krout et al., 2002). Table 3 provides a list of structures afferent to the mammalian SCN that correspond to structures identified in the chick. As was indicated with efferents, afferent structures to the mSCN and vSCN are more numerous than is the case in the mammalian SCN. Figure 9 provides a schematic representation of rodent and chicken afferents.

The reception of afferents from SL completes a circuit between that structure and mSCN. Input to the mSCN from SL is corroborated by a study of efferents traced from that structure (Montagnese et al., 2004). A similar bidirectional interaction with SL exists in rats (Moga and Moore, 1997; Leak and Moore, 2001; Krout et al., 2002). While nBST is not an afferent structure of the rodent SCN, its afferent input to the chick mSCN supports the hypothesis that encephalic photoreceptors of the LSO project indirectly to the mSCN. The mSCN also receives afferent input from hypothalamic structures apposed to the periventricular organ (PVO), another putative encephalic photoreceptive structure (cf. Silver et al., 1988), suggesting another putative pathway by which light information may reach the avian suprachiasmatic nucleus.

As is the case in the mammalian SCN, the primary afferent to the vSCN is the retina. In mammals, some light information is carried to the SCN from the geniculate nuclei and intergeniculate leaflet (IGL) via the geniculohypothalamic tract (Card and Moore, 1982, 1989; Moore et al., 1984; Harrington et al., 1985; Moore and Speh, 1993; Moore and Card, 1994). Our data suggest a similar relationship between the perirotundal area, which is homologous to the mammalian IGL (Gunturkun and Karten, 1991), the geniculate nuclei and the vSCN. Further, the nuclei of the pretectal area project to the rat SCN (Mikkelsen and Vrang, 1994), while, in the chick, many pretectal and visually active thalamic structures project to the vSCN, indicating an abundant afferent input to the vSCN by structures of the tectofugal, thalamofugal and accessory optic pathways. A few structures associated with the tectofugal and thalamofugal pathways also project to the mSCN, suggesting a minor modulatory role in its function.

Taken together, mSCN and vSCN afferents are very similar to the afferents of the mammalian SCN. As is seen with the core and shell of the mammalian SCN, there is significant overlap between the connections of the two avian structures.

Connections between mSCN and vSCN

We found that the mSCN and vSCN communicate bidirectionally and bilaterally. Projections from the vSCN to the mSCN are stronger than they are in the converse. In rodents, the core of the SCN communicates with the shell, but the shell doesn't send efferents to the core (Abrahamson and Moore, 2001). Thus, although the details of the relationship between putative sub-regions of the avian suprachiasmatic complex are different than the situation in the mammalian circadian system, the general scheme suggests an asymmetric flow of retinal information from the vSCN to the mSCN. This scheme is generally similar to the relationship of the "core" and "shell" of the rodent SCN.

Evaluation of projections based on misplaced injections

Assessment of efferent connections was made possible by several injections. In the region dorsal to the mSCN, we found that AM has several common efferents with mSCN. An injection that encompassed the dorsal mSCN and the ventral aspect of AM identified an efferent population that is an amalgam of the two structures' efferents. Interestingly, several of the efferents common to the mSCN and mSCN/AM are more abundant when traced from the more dorsal injection site, most notably SL, nBSTL and the habenula. There are several possible explanations. First, more abundant projections may arise from the dorsal mSCN. Second, the presence of BDA in two structures with common targets may have had an additive effect. Finally, AM may be involved in multisynaptic pathways originating in or involving the mSCN. The fact that ventral mSCN injection labels AM supports the third hypothesis, although all three possibilities may be responsible for the greater abundance of stain in mSCN/AM injections. In mammals, one structure involved in such pathways is the subparaventricular zone (SPZ), which is just dorsal to the SCN. The mammalian SCN sends

a considerable efferent projection to the SPZ, which then sends efferents to a variety of downstream structures. Thus, injection to SPZ often results in an efferent pattern similar to SCN, but with more abundant terminal fibers present in those structures (Watts et al., 1991). The data presented here imply that a similar, albeit less intense, relationship may exist between mSCN and the region immediately dorsal to mSCN, perhaps including AM. This possibility is made all the more intriguing by the presence of sparse retinal terminals in and between the two structures. By way of contrast, injection to the gray matter just dorsal to the vSCN does not produce any amplification of efferent abundance, although the structures receiving efferents from this injection are very similar to those obtained from vSCN injections. This similarity of efferent staining is probably at least partially due to uptake by efferent fibers of the vSCN.

In studies of suprachiasmatic afferents, misplaced injections again serve an important role in the analysis of our results. A large CTB injection that included the entirety of AM and the dorsal portion of mSCN transported to an afferent population very similar to what was found in the ventral mSCN injections. None of the injections were delivered to AM only; however, based on efferent findings, one may reasonably suspect that the more lateral thalamic afferents are those of AM itself. In contrast to what was found in the efferent study, some afferent projections are stronger when traced from mSCN alone and some stained more abundantly after injection to AM/mSCN. This suggests that, if AM is involved in mSCN-mediated communication, 1) it is only involved in this capacity with a subset of structures and 2) it is more active in the relay of efferent messages than in the reception of afferent signals. Because we may only speculate given the data here, studies designed to determine the precise relationship between AM and mSCN are necessary in the exploration of the suprachiasmatic nucleus of birds.

Our missed injections were able to confirm a few efferent and afferent projections reported based on mSCN and vSCN injection. First, injection of BDA into AM led to efferent staining in mSCN, supporting our finding that there are cells afferent to mSCN within that nucleus. Second, injection of CTB into POA confirmed mSCN efferents to that structure. Third, injection of CTB to ICT confirmed its reception of vSCN efferents. Finally, CTB injections contained within GLv resulted in a large fiber plexus within vSCN. While we did not choose to report efferent projections from CTB injections, opting to use BDA instead, no BDA injections were placed in the GLv, so we used the CTB injections for confirmation of geniculohypothalamic fibers to the vSCN (Fig. 1W). Reciprocal injection to other efferents and afferents will be necessary to assess their full extent and validity.

Functional comparisons of the mSCN and vSCN

Lesion studies support the involvement of the mSCN in expression of circadian locomotor rhythms. Initial lesions of the anterior hypothalamus resulted in loss of locomotor activity rhythms in house sparrows (Takahashi and Menaker, 1982), Japanese quail (Simpson and Follett, 1981) and Java sparrows (Ebihara and Kawamura, 1981). These lesions comprised a large portion of the anterior hypothalamus, likely destroying both the mSCN and vSCN. To resolve this issue, Ebihara et al. (1987) produced individual lesions to the vSCN and mSCN in pigeons; these lesions, by themselves, had little effect. However, lesions of the mSCN in pigeons that had also received either pinealectomy or enucleation (each of which only disrupts rhythmicity) abolished or further disrupted free running rhythms in constant dim light (dimLL). Lesions of the vSCN failed to abolish free running rhythms in dimLL. In contrast, Cassone et al. (1990) found that specific lesions in the vSCN abolished circadian patterns of norepinephrine turnover in the chick pineal gland, but that lesions of mSCN had no effect on this output.

Conversely, physiological analyses of rhythmic function points to the vSCN as a circadian oscillator. The vSCN, but not the mSCN, of the house sparrow exhibits circadian rhythms of 2-deoxy[^{14}C]glucose (2DG) uptake, such that 2DG uptake is high during the subjective day and low during the subjective night (Cassone, 1988; Lu and Cassone, 1993a). In the chick, 2DG uptake is rhythmic in constant darkness in both structures (Cantwell and Cassone, 2002), such that uptake is highest during subjective day. This phase of peak uptake is similar to the situation in the mammalian SCN (Schwartz et al. 1980). In Japanese quail, the vSCN exhibits rhythmic electrical activity *in vitro* (Juss et al., 1994), with activity greater during the subjective day, also similar to the situation for the mammalian SCN (Green and Gillette, 1982). Finally, the early immediate gene *c-fos*, which is induced in the mammalian SCN by a one-hour light pulse during the night (Rea, 1989), is similarly induced in the vSCN, but not in the mSCN, of quail and starlings (King and Follett, 1997).

Of course, the role of an avian SCN must be integrally linked to the role of pineal melatonin in circadian organization (Cassone, 1998), and the vSCN fits this criterion rather well. First, exogenous melatonin administration during the day acutely inhibits 2DG uptake in the vSCN, but not the mSCN, of sparrows (Cassone and Brooks, 1991) and chickens (Cantwell and Cassone, 2002). This is similar to the situation in rodents (Cassone et al., 1988a). Secondly, pinealectomy of house sparrows not only abolishes circadian locomotor patterns but also abolishes the circadian rhythms of 2DG uptake in the vSCN (Lu and Cassone, 1993a). Thirdly, rhythmic administration of melatonin to arrhythmic, pinealectomized sparrows restores both a rhythm of locomotion and a rhythm of 2DG uptake in the vSCN, but not the mSCN, such that 2DG uptake is lower during melatonin administration than during vehicle administration (Lu et al., 1993b). Finally, the vSCN of more than 20 species of birds express high density, high affinity binding of radiolabeled 2-[^{125}I]-iodomelatonin (IMEL) (Rivkees et al., 1989; Stehle, 1990; Cassone and Brooks, 1991; Siuciak et al., 1991; Brooks and Cassone, 1992; Cassone et al., 1995). The mSCN do not.

Recent advances in the molecular biology of circadian clocks have offered yet another avenue for the comparative study of the SCN. In rodents, several transcription factors and kinases, labeled “clock genes”, are involved in a complex transcriptional-translational feedback loop that is at the core of a model explaining the generation of biological rhythms (Reppert and Weaver, 2002). Included in this loop are *period* genes (*pers*), *cryptochromes* (*crys*), *clock*, *bmal1* and *E4bp4*, which have been identified within the mammalian SCN (cf. Hastings and Herzog, 2004). Avian orthologs for these genes have been identified (Bailey et al., 2003, 2004). Several of these genes have been identified in the mSCN but not the vSCN in Japanese quail (Yoshimura et al. 2001; Yasuo et al., 2003). In the house sparrow, *pPer2* expression is rhythmic in both the mSCN and the vSCN such that it is highest during the mid-day (Brandstatter et al., 2001), which is similar to the phasing seen in the mouse SCN (Tei et al. 1997).

A working model of the avian SCN

The present data and literature suggest to us that there is a role for both the mSCN and the vSCN in the avian circadian system. As with the pineal and the retinae, these structures will likely have varying levels of importance in different avian species. We hypothesize that both the mSCN and the vSCN are involved in a suprachiasmatic complex that serves as a functional equivalent of the mammalian SCN. At this stage, attribution of “homology” to these structures is premature. Further developmental and more comparative analyses of extant amniote vertebrate species will be necessary to truly address this issue.

Our model (Fig. 10) states that light information is transmitted to the suprachiasmatic complex via three separate input pathways. The first of these is the retinohypothalamic tract (RHT), which has been well characterized in the vSCN of many avian species. Sparse RHT

input also transmits light information to the mSCN. The second photic input to the vSCN is indirect, through the perirotundal area and geniculate nuclei via a pathway homologous to the mammalian GHT, described above. The third and final light input to our suprachiasmatic complex is input to the mSCN via the encephalic photoreceptors of LSO and PVO. While sufficient data has not been produced to bear out the existence of a specific connection, the hypothesis is supported by the finding of Yoshimura et al. (2001) that a one-hour light pulse during the subjective night is capable of inducing *per2* RNA expression in the mSCN of quail whose eyes are covered by opaque black rubber caps, barring RHT and GHT transduction of the signal. The possibility that such a light input exists is intriguing given the finding that melanopsin protein is expressed in the lateral septal region, as well as the hypothalamic periventricular region (Chaurasia et al., 2005). The mSCN and vSCN have bilateral and bidirectional communication, allowing them to share light information with one another.

Both the mSCN and vSCN have been implicated in the literature as circadian pacemakers. Our model suggests that the mSCN drives locomotor activity and body temperature rhythms, based on lesion studies (Ebihara et al., 1987; Yoshimura et al., 2001). Conversely, we propose that the vSCN regulates choroidal blood flow via EWm, drives and/or entrains circadian rhythms of visual function and regulates pineal melatonin secretion via the sympathetic nervous system. As was shown in this study, there is abundant connectivity between the vSCN and structures of the thalamofugal, tectofugal and accessory optic visual pathways.

Why are there two structures in birds undertaking the role of the mammalian SCN? We hypothesize that the evolution of this organization involves the development of the supraoptic decussation, which is extensive in birds and first visible in the chick on embryonic day 8 (E8). By E15, it is quite thick and has visible subdivisions (Ehrlich et al., 1988). The retinohypothalamic innervation of the hypothalamus, on the other hand, is not visible until E15 or E16 (Shimizu et al., 1984). We propose that, because of the conflicting developmental timing of the supraoptic decussation and RHT, significant mSCN innervation by retinohypothalamic terminals is not physically permitted. Instead, retinal afferents innervate the vSCN, which in turn innervate the mSCN. If this is the case, this anatomical configuration may be a derived feature and unique to birds, which express a greater inter-hemispheric interaction of visual information than do other taxa (Ehrlich et al., 1988) with the possible exception of crocodilians (Crosby and Showers, 1969). If this is the case, then we might expect a similar organization in crocodilians as birds, which share archosaurian ancestry (Rogers, 1999), although the SCN of other reptile taxa are more similar in location to the mammalian SCN (Tosini et al., 2001). Clearly, more comparative research on non-mammalian vertebrates will be required to test this hypothesis.

Further, analysis of the chemoarchitecture of these two structures in this and other avian species will be important in understanding avian circadian organization as well as the evolution of the diencephalons. More detailed studies of the development of the retinohypothalamic tract in birds and other non-mammalian vertebrates may provide a clearer view of suprachiasmatic nucleus function and evolution.

Acknowledgments

This work was supported by NIH PO1 NS39546 to VMC.

The authors wish to thank Barbara Earnest and her vivarium staff for their care of the chickens used in these experiments. We thank Victor Johnson of our departmental Instrument shop for keeping our Midgard power supply up and running for the duration of the experiment. We also thank Dr. David Earnest for the Alexa Fluor 594-

conjugated CTB. We thank Dr. Paul Bartell for his comments and suggestions. Finally, thanks to Lily Bartoszek and Drs. Jim Golden, Susan Golden and Mark Zoran for technological assistance.

LITERATURE CITED

Abrahamson EE, Moore RY. Suprachiasmatic nucleus in the mouse: retinal innervation, intrinsic organization and efferent projections. Brain Res. 2001; 916:172–191. [PubMed: 11597605]

Adachi A, Hasegawa M, Ebihara S. Measurement of circadian rhythms of ocular melatonin in the pigeon by *in vivo* microdialysis. NeuroReport. 1995; 7:286–288. [PubMed: 8742471]

Bailey MJ, Cassone VM. Melanopsin expression in the chick retina and pineal gland. Mol Brain Res. 2005; 134:345–348. [PubMed: 15836930]

Bailey MJ, Beremand PD, Hammer R, Bell-Pedersen D, Thomas TL, Cassone VM. Transcriptional profiling of the chick pineal gland, a photoreceptive circadian oscillator and pacemaker. Mol Endocrinol. 2003; 17:2084–2095. [PubMed: 12881511]

Bailey MJ, Beremand PD, Hammer R, Reidel E, Thomas TL, Cassone VM. Transcriptional profiling of circadian patterns of mRNA expression in the chick retina. J Biol Chem. 2004; 279:52247–52254. [PubMed: 15448147]

Binkley S, Hryshchyshyn M, Reilly K. N-acetyltransferase activity responds to environmental lighting in the eye as well as in the pineal gland. Nature. 1979; 281:479–481. [PubMed: 492306]

Bons N. Retinohypothalamic pathway in the duck (*Anas platyrhynchos*). Cell Tissue Res. 1976; 168:343–360. [PubMed: 1277273]

Brandstatter R, Abraham U, Albrecht U. Initial demonstration of rhythmic *Per* gene expression in the hypothalamus of a non-mammalian vertebrate, the house sparrow. Neuroreport. 2001; 12:1167–1170. [PubMed: 11338185]

Brooks DS, Cassone VM. Daily and circadian regulation of 2-[125]iodomelatonin binding in the chick brain. Endocrinology. 1992; 131:1297–1304. [PubMed: 1324157]

Calaza KC, Gardino PF. Evidence of muscarinic acetylcholine receptors in the retinal centrifugal system of the chick. Braz J Med Biol Res. 2000; 33:1075–1082. [PubMed: 10973141]

Cantwell EL, Cassone VM. Daily and circadian fluctuation in 2-deoxy[(14)C]-glucose uptake in circadian and visual system structures of the chick brain: effects of exogenous melatonin. Brain Res Bull. 2002; 57:603–611. [PubMed: 11927362]

Card JP, Moore RY. Ventral lateral geniculate nucleus efferents to the rat suprachiasmatic nucleus exhibit avian pancreatic polypeptide-like immunoreactivity. J Comp Neurol. 1982; 206:390–396. [PubMed: 6178763]

Card JP, Moore RY. Organization of lateral geniculate-hypothalamic connections in the rat. J Comp Neurol. 1989; 284:135–147. [PubMed: 2754028]

Cassone VM. Circadian variation of [14C]2-deoxyglucose uptake within the suprachiasmatic nucleus of the house sparrow *Passer domesticus*. Brain Res. 1988; 30;459:178–182. [PubMed: 3167578]

Cassone VM. Melatonin's role in vertebrate circadian rhythms. Chronobiol Int. 1998; 15:457–473. [PubMed: 9787936]

Cassone VM, Brooks DS. Sites of melatonin action in the brain of the house sparrow, *Passer domesticus*. J Exp Zool. 1991; 260:302–309.

Cassone VM, Moore RY. Retinohypothalamic projection and suprachiasmatic nucleus of the house sparrow, *Passer domesticus*. J Comp Neurol. 1987; 266:171–182. [PubMed: 3437073]

Cassone VM, Brooks DS, Kelm TA. Comparative distribution of 2[125]Iodomelatonin binding in the brains of diurnal birds—outgroup analysis with turtles. Brain Behav Evol. 1995; 45:241–256. [PubMed: 7620873]

Cassone VM, Forsyth AM, Woodlee GL. Hypothalamic regulation of circadian noradrenergic input to the chick pineal gland. J Comp Physiol A. 1990; 167:187–192. [PubMed: 1976805]

Cassone VM, Roberts MH, Moore RY. Effects of melatonin on 2-deoxy-[1-14C]glucose uptake within rat suprachiasmatic nucleus. Am J Physiol. 1988a; 255:R332–337. [PubMed: 3407806]

Cassone VM, Speh JC, Card JP, Moore RY. Comparative anatomy of the mammalian hypothalamic suprachiasmatic nucleus. J Biol Rhythms. 1988b; 3:71–91. [PubMed: 2979633]

Chabot CC, Menaker M. Feeding rhythms in constant light and constant darkness: the role of the eyes and the effect of melatonin infusion. J Comp Physiol A. 1994; 175:75–82. [PubMed: 8083848]

Chaurasia SS, Rollag MD, Jiang G, Hayes WP, Haque R, Natesan A, Zatz M, Tosini G, Liu C, Korf HW, Iuvone PM, Provencio I. Molecular cloning, localization and circadian expression of chicken melanopsin (*Opn4*): differential regulation of expression in pineal and retinal cell types. J Neurochem. 2005; 92:158–170. [PubMed: 15606905]

Chen S, Aston-Jones G. Evidence that cholera toxin B subunit (CTb) can be avidly taken up and transported by fibers of passage. Brain Res. 1995; 674:107–111. [PubMed: 7773677]

Chen Y, Naito J. Morphological classification of ganglion cells in the central retina of chicks. J Vet Med Sci. 1999; 61:537–542. [PubMed: 10379947]

Chou TC, Bjorkum AA, Baus SE, Lu J, Scammell TE, Saper CB. Afferents to the ventrolateral preoptic nucleus. J Neurosci. 2002; 22:977–990. [PubMed: 11826126]

Cooper ML, Pickard GE, Silver R. Retinohypothalamic pathway in the dove demonstrated by anterograde HRP. Brain Res Bull. 1983; 10:715–718. [PubMed: 6871740]

Crosby, EL.; Showers, MJL. Comparative anatomy of the preoptic and hypothalamic areas. In: Haymaker, W.; Anderson, E.; Nauta, WJH., editors. The Hypothalamus. Springfield, Illinois; ChC Thomas: 1969. p. 61-135.

Dai J, Swaab DF, Van der Vliet J, Buijs RM. Postmortem tracing reveals the organization of hypothalamic projections of the suprachiasmatic nucleus in the human brain. J Comp Neurol. 1998; 400:87–102. [PubMed: 9762868]

Drucker-Colin R, Aguilar-Roblero R, Garcia-Hernandez F, Fernandez-Cancino F, Bermudez-Rattoni F. Fetal suprachiasmatic nucleus transplants: Diurnal rhythm recovery of lesioned rats. Brain Res. 1984; 311:353–357. [PubMed: 6541955]

Ebihara S, Kawamura H. The role of the pineal organ and the suprachiasmatic nucleus in the control of circadian locomotor rhythms in the Java sparrow, *Padda oryzivora*. J Comp Physiol. 1981; 141:207–214.

Ebihara, S.; Oshima, I.; Yamada, H.; Goto, M.; Sato, K. Circadian organization in the pigeon. In: Hiroshige, T.; Honma, K., editors. Comparative Aspects of Circadian Clocks. Sapporo; Hokkaido UP: 1987. p. 88-94.

Ebihara S, Uchiyama K, Oshima I. Circadian organization in the pigeon, *Columba livia*: the role of the pineal organ and the eye. J Comp Physiol. 1984; 154:59–69.

Ehrlich D, Mark R. An atlas of the primary visual projections in the brain of the chick *Gallus gallus*. J Comp Neurol. 1984; 223:592–610. [PubMed: 6325511]

Ehrlich D, Zappia JV, Saleh CN. Development of the supraoptic decussation in the chick (*Gallus gallus*). Anat Embryol (Berl). 1988; 177:361–370. [PubMed: 3354852]

Fitzgerald MEC, Vana BA, Reiner A. Control of choroidal blood flow by the nucleus of Edinger-Westphal in pigeons: a laser Doppler study. Invest Ophthalmol Vis Sci. 1990; 31:2483–2492. [PubMed: 2265988]

Gamlin PD, Cohen DH. Retinal projections to the pretectum in the pigeon (*Columba livia*). J Comp Neurol. 1988; 269:1–17. [PubMed: 3360999]

Gamlin PD, Reiner A, Karten HJ. Substance P-containing neurons of the avian suprachiasmatic nucleus project directly to the nucleus of Edinger-Westphal. Proc Natl Acad Sci USA. 1982; 79:3891–3895. [PubMed: 6179091]

Gardino PF, Schmal AR, Calaza KC. Identification of neurons with acetylcholinesterase and NADPH-diaphorase activities in the centrifugal visual system of the chick. J Chem Neuroanat. 2004; 27:267–273. [PubMed: 15261333]

Gooley JJ, Lu J, Fischer D, Saper CB. A broad role for melanopsin in nonvisual photoreception. J Neurosci. 2003; 23:7093–7106. [PubMed: 12904470]

Green DJ, Gillette R. Circadian rhythm of firing rate recorded from single cells in the rat suprachiasmatic nucleus brain slice. Brain Res. 1982; 245:198–200. [PubMed: 6889453]

Groos G, Hendriks J. Circadian rhythms in electrical discharge of rat suprachiasmatic neurons recorded *in vitro*. Neurosci Lett. 1982; 34:283–288. [PubMed: 6298675]

Güntürkün O, Karten HJ. An immunocytochemical analysis of the lateral geniculate complex in the pigeon (*Columba livia*). J Comp Neurol. 1991; 314:721–749. [PubMed: 1687743]

Hamm HE, Menaker M. Retinal rhythms in chicks: circadian variation in melatonin and serotonin N-acetyltransferase activity. Proc Natl Acad Sci USA. 1980; 77:4998–5002. [PubMed: 6933543]

Harrington ME, Nance DM, Rusak B. Neuropeptide Y immunoreactivity in the hamster geniculo-suprachiasmatic tract. Brain Res Bull. 1985; 15:465–472. [PubMed: 3840718]

Hartwig HG. Electron microscopic evidence for a retinohypothalamic projection to the suprachiasmatic nucleus of *Passer domesticus*. Cell Tissue Res. 1974; 153:89–99. [PubMed: 4442081]

Hastings MH, Herzog ED. Clock genes, oscillators, and cellular networks in the suprachiasmatic nuclei. J Biol Rhythms. 2004; 19:400–413. [PubMed: 15534320]

Inouye ST, Kawamura H. Persistence of circadian rhythmicity in a mammalian hypothalamic "island" containing the suprachiasmatic nucleus. Proc Natl Acad Sci USA. 1979; 76:5962–5966. [PubMed: 293695]

Juss TS, Davies IR, Follett BK, Mason R. Circadian rhythm in neuronal discharge activity in the quail lateral hypothalamic retinorecipient nucleus (LHRN) recording *in vitro*. J Physiol. 1994; 485:132.

Kalsbeek A, Teclemariam-Mesbah R, Pevet P. Efferent projections of the suprachiasmatic nucleus in the golden hamster (*Mesocricetus auratus*). J Comp Neurol. 1993; 332:293–314. [PubMed: 8331217]

King VM, Follett BK. c-fos expression in the putative avian suprachiasmatic nucleus. J Comp Physiol A. 1997; 180:541–551. [PubMed: 9163930]

Klein DC, Moore RY. Pineal N-acetyltransferase and hydroxyindole-O-methyltransferase: control by the retinohypothalamic tract and the suprachiasmatic nucleus. Brain Res. 1979; 174:245–262. [PubMed: 487129]

Kriegsfeld LJ, Leak RK, Yackulic CB, LeSauter J, Silver R. Organization of suprachiasmatic nucleus projections in Syrian hamsters (*Mesocricetus auratus*): an anterograde and retrograde analysis. J Comp Neurol. 2004; 468:361–379. [PubMed: 14681931]

Krout KE, Kawano J, Mettenleiter TC, Loewy AD. CNS inputs to the suprachiasmatic nucleus of the rat. Neurosci. 2002; 110:73–92.

Kuenzel WJ. The search for deep encephalic photoreceptors within the avian brain, using gonadal development as a primary indicator. Poult Sci. 1993; 72:959–967. [PubMed: 8502618]

Kuenzel, WJ.; Masson, M. A Stereotaxic Atlas of the Brain of the Chick (*Gallus domesticus*). Baltimore, Maryland: The Johns Hopkins University Press; 1988.

Kuenzel WJ, van Tienhoven A. Nomenclature and location of avian hypothalamic nuclei and associated circumventricular organs. J Comp Neurol. 1982; 206:293–313. [PubMed: 7085935]

Leak RK, Moore RY. Topographic organization of suprachiasmatic nucleus projection neurons. J Comp Neurol. 2001; 433:312–334. [PubMed: 11298358]

Lehman MN, Silver R, Gladstone WR, Kahn RM, Gibson M, Bittman EL. Circadian rhythmicity restored by neural transplant. Immunocytochemical characterization of the graft and its integration with the host brain. J Neurosci. 1987; 6:1626–1638. [PubMed: 3598638]

Li H, Ferrari MB, Kuenzel WJ. Light-induced reduction of cytoplasmic free calcium in neurons proposed to be encephalic photoreceptors in chick brain. Brain Res Dev Brain Res. 2004; 153:153–161.

Lu J, Cassone VM. Pineal regulation of circadian rhythms of 2-deoxy[^{14}C]glucose uptake and 2[^{125}I]iodomelatonin binding in the visual system of the house sparrow, *Passer domesticus*. J Comp Physiol A. 1993a; 173:765–774.

Lu J, Cassone VM. Daily melatonin administration synchronizes circadian patterns of brain metabolism and behavior in pinealectomized house sparrows, *Passer domesticus*. J Comp Physiol A. 1993b; 173:775–782.

Lu J, Shiromani P, Saper CB. Retinal input to the sleep-active ventrolateral preoptic nucleus in the rat. Neurosci. 1999; 93:209–214.

McGoogan JM, Cassone VM. Circadian regulation of chick eletroretinogram: effects of pinealectomy and exogenous melatonin. Am J Physiol. 1999; 277:R1418–1427. [PubMed: 10564215]

Meier RE. Autoradiographic evidence for a direct retinohypothalamic projection in the avian brain. Brain Res. 1973; 53:417–421. [PubMed: 4122358]

Menaker, M.; Tosini, G. The evolution of vertebrate circadian systems. In: Honma, K.; Honma, S., editors. Proceedings of the Sixth Sapporo Symposium on Biological Rhythms. Sapporo: Hokkaido University Press; 1995. p. 39-52.

Mey J, Johann V. Dendrite development and target innervation of displaced retinal ganglion cells of the chick (*Gallus gallus*). Int J Devl Neuroscience. 2001; 19:517–531.

Mikkelson JD, Vrang N. A direct pretectosuprachiasmatic projection in the rat. Neuroscience. 1994; 62:497–505. [PubMed: 7530345]

Moga MM, Moore RY. Organization of neural inputs to the suprachiasmatic nucleus in the rat. J Comp Neurol. 1997; 389:508–534. [PubMed: 9414010]

Montagnese CM, Szekely AD, Adam A, Csillag A. Efferent connections of septal nuclei of the domestic chick (*Gallus domesticus*): an anterograde pathway tracing study with a bearing on functional circuits. J Comp Neurol. 2004; 469:437–456. [PubMed: 14730592]

Moore RY. Retinohypothalamic projection in mammals: a comparative study. Brain Res. 1973; 49:403–409. [PubMed: 4124397]

Moore, RY. The retinohypothalamic tract, suprachiasmatic hypothalamic nucleus and central neural mechanisms of circadian rhythm regulation. In: Suda, M.; Hayashi, O.; Hakagawa, H., editors. Biological Rhythms and Their Central mechanism. Amsterdam: Elsevier/North Holland Press; 1979. p. 343-354.

Moore RY, Card JP. Intergeniculate leaflet: an anatomically and functionally distinct subdivision of the lateral geniculate complex. J Comp Neurol. 1994; 344:403–430. [PubMed: 8063960]

Moore RY, Eichler VB. Loss of a circadian adrenal corticosterone rhythm following suprachiasmatic lesions in the rat. Brain Res. 1972; 42:201–206. [PubMed: 5047187]

Moore RY, Klein DC. Visual pathways and the central neural control of a circadian rhythm in pineal serotonin N-acetyltransferase activity. Brain Res. 1974; 10:17–33. [PubMed: 4595289]

Moore RY, Lenn NJ. A retinohypothalamic projection in the rat. J Comp Neurol. 1972; 146:1–14. [PubMed: 4116104]

Moore RY, Speh JC. GABA is the principal neurotransmitter of the circadian system. Neurosci Lett. 1993; 150:112–116. [PubMed: 8097023]

Moore RY, Gustafson EL, Card JP. Identical immunoreactivity of afferents to the rat suprachiasmatic nucleus with antisera against avian pancreatic polypeptide, molluscan cardioexcitatory peptide and neuropeptide Y. Cell Tissue Res. 1984; 236:41–46. [PubMed: 6201281]

Moore RY, Karapas F, Lenn NJ. A retinohypothalamic projection in the rat. Anat Rec. 1971; 169:382–383.

Moore RY, Speh JC, Leak RK. Suprachiasmatic nucleus organization. Cell Tissue Res. 2002; 309:89–98. [PubMed: 12111539]

Morin LP, Goodless-Sanchez N, Smale L, Moore RY. Projections of the suprachiasmatic nuclei, subparaventricular zone and retrochiasmatic area in the golden hamster. Neuroscience. 1994; 61:391–410. [PubMed: 7526267]

Natesan AJ, Geetha L, Zatz M. Rhythm and soul in the avian pineal. Cell Tissue Res. 2002; 309:35–45. [PubMed: 12111535]

Newman GC, Hospod FE, Patlak CS, Moore RY. Analysis of *in vitro* glucose utilization in a circadian pacemaker model. J Neurosci. 1992; 12:2015–2021. [PubMed: 1607926]

Norgren RB, Silver R. Retinohypothalamic projections and the suprachiasmatic nucleus in birds. Brain Behav Evol. 1989; 34:73–83. [PubMed: 2819412]

Nyce J, Binkley S. Extraretinal photoreception in chickens: entrainment of the circadian locomotor activity rhythm. Photochem Photobiol. 1977; 25:529–531. [PubMed: 896964]

Oliver J, Bouillé C, Herbuté S, Baylé JD. Retrograde transport from the preoptic-anterior hypothalamic region to retinal ganglion cells in quail. Neurosci Lett. 1978; 9:291–295. [PubMed: 19605234]

Oshima I, Yamada H, Goto M, Sato K, Ebihara S. Pineal and retinal melatonin is involved in the control of circadian locomotor and body temperature rhythms in the pigeon. J Comp Physiol A. 1989; 166:217–226.

Pickard GE. The afferent connections of the suprachiasmatic nucleus of the golden hamster with emphasis on the retinohypothalamic projection. J Comp Neurol. 1982; 211:65–83. [PubMed: 7174884]

Rathinam T, Kuenzel WJ. Attenuation of gonadal response to photostimulation following ablation of neurons in the lateral septal organ of chicks. Brain Res Bull. 2005; 64:455–461. [PubMed: 15607834]

Rea MA. Light increases Fos-related protein immunoreactivity in the rat suprachiasmatic nuclei. Brain Res Bull. 1989; 23:577–581. [PubMed: 2514963]

Reiner A, Fitzgerald MED, Gamlin PDR. Central neural circuits controlling choroidal blood flow: a laser-Doppler study. Invest Ophthalmol Vis Sci Suppl. 1990; 31:38.

Reiner A, Perkel DJ, Bruce LL, Butler AB, Csillag A, Kuenzel W, Medina L, Paxinos G, Shimizu T, Striedter G, Wild M, Ball GF, Durand S, Gunturkun O, Lee DW, Mello CV, Powers A, White SA, Hough G, Kubikova L, Smulders TV, Wada K, Dugas-Ford J, Husband S, Yamamoto K, Yu J, Siang C, Jarvis ED. Revised nomenclature for avian telencephalon and some related brainstem nuclei. J Comp Neurol. 2004; 473:377–414. [PubMed: 15116397]

Reppert SM, Weaver DR. Coordination of circadian timing in mammals. Nature. 2002; 418:935–941. [PubMed: 12198538]

Rivkees SA, Cassone VM, Weaver DR, Reppert SM. Melatonin receptors in chick brain: characterization and localization. Endocrinology. 1989; 125:363–368. [PubMed: 2544407]

Rogers SW. Allosaurus, crocodiles, and birds: evolutionary clues from spiral computed tomography of an endocast. Anat Rec. 1999; 257:162–173. [PubMed: 10597341]

Sawaki Y, Nihonmatsu I, Kawamura H. Transplantation of the neonatal suprachiasmatic nuclei into rats with complete bilateral suprachiasmatic lesions. Neurosci Res. 1984; 1:67–72. [PubMed: 6536887]

Schwartz WJ, Davidsen LC, Smith CB. *In vivo* metabolic activity of a putative circadian oscillator, the rat suprachiasmatic nucleus. J Comp Neurol. 1980; 189:157–167. [PubMed: 7351445]

Schwartz WJ, Gainer H. Suprachiasmatic nucleus: use of 14C-labeled deoxyglucose uptake as a functional marker. Science. 1977; 197:1089–1091. [PubMed: 887940]

Sherin JE, Elmquist JK, Torrealba F, Saper CB. Innervation of histaminergic tuberomammillary neurons by GABAergic and galaninergic neurons in the ventrolateral preoptic nucleus of the rat. J Neurosci. 1998; 15:4705–4721. [PubMed: 9614245]

Shibata S, Oomura Y, Kita H, Hattori H. Circadian rhythmic changes of neuronal activity in the suprachiasmatic nucleus of the rat hypothalamic slice. Brain Res. 1982; 247:154–158. [PubMed: 7127113]

Shimizu T, Cox K, Harvey JK, Britto LRG. Cholera toxin mapping of retinal projections in pigeons (*Columba livia*), with emphasis on retinohypothalamic connections. Vis Neurosci. 1994; 11:441–446. [PubMed: 8038120]

Shimizu I, Yoshimoto M, Kojima T, Okadao N. Development of retinohypothalamic projections in the chick embryo. Neurosci Lett. 1984; 50:43–47. [PubMed: 6493638]

Silver R, Witkovsky P, Horvath P, Alones V, Barnstable CJ, Lehman MN. Coexpression of opsin- and VIP-like-immunoreactivity in CSF-contacting neurons of the avian brain. Cell Tissue Res. 1988; 253:189–198. [PubMed: 2970894]

Simpson SM, Follett BK. Pineal and hypothalamic pacemakers: their role in regulating circadian rhythmicity in the Japanese quail. J Comp Physiol A. 1981; 144:381–389.

Siuciak JA, Drause DN, Dubocovich ML. Quantitative pharmacological analysis of 2-^{125}I-iodomelatonin binding sites in discrete areas of the chicken brain. J Neurosci. 1991; 11:2855–2864. [PubMed: 1652626]

Stehle J. Melatonin binding sites in brain of the 2-day-old chicken: an autoradiographic localisation. J Neural Transm Gen Sect. 1990; 81:83–89. [PubMed: 2162678]

Stephan FK, Berkley KJ, Moss RL. Efferent connections of the rat suprachiasmatic nucleus. Neuroscience. 1981; 6:2625–2641. [PubMed: 7322354]

Stephan FK, Zucker I. Circadian rhythms in drinking behavior and locomotor activity of rats are eliminated by hypothalamic lesions. Proc Natl Acad Sci USA. 1972; 69:1583–1586. [PubMed: 4556464]

Takahashi JS, Menaker M. Role of the suprachiasmatic nucleus in the circadian system of the house sparrow. J Neurosci. 1982; 2:815–828. [PubMed: 7086486]

Tei H, Okamura H, Shigeyoshi Y, Fukuhara C, Ozawa R, Irose M, Sakaki Y. Circadian oscillation of a mammalian homologue of the *Drosophila period* gene. Nature. 1997; 389:512–516. [PubMed: 9333243]

Tombol T, Eyre M, Zayats N, Nmeth A. The ramifications and terminals of optic fibres in layers 2 and 3 of the avian optic tectum: a Golgi and light and electron microscopic anterograde tracer study. Cells Tissues Organs. 2003; 175:202–222. [PubMed: 14707401]

Tosini G, Bertolucci C, Foa A. The circadian system of reptiles: a multioscillatory and multiphotoreceptive system. Physiol Behav. 2001; 72:461–471. [PubMed: 11282129]

Uchiyama H. Centrifugal pathways to the retina: influence of the optic tectum. Vis Neurosci. 1989; 3:183–206. [PubMed: 2487102]

Underwood H, Siopes T. Circadian organization in Japanese quail. J Exp Zool. 1984; 232:557–566. [PubMed: 6520587]

van Tienhoven A, Jühász LW. The chicken telencephalon, diencephalon and mesencephalon in stereotaxic coordinates. J Comp Neurol. 1962; 118:185–198. [PubMed: 13924637]

Veenman CL, Reiner A, Honig MG. Biotinylated dextran amine as an anterograde tracer for single- and double-labeling studies. J Neurosci Methods. 1992; 41:239–254. [PubMed: 1381034]

Vigh-Teichmann I, Rohlich P, Vigh B, Aros B. Comparison of pineal complex, retina and cerebrospinal fluid contacting neurons by immunocytochemical antirhodopsin reaction. Z Mikrosk Anat Forsch. 1980; 94:623–640. [PubMed: 7456628]

Wallman J, Saldanha CJ, Silver R. A putative suprachiasmatic nucleus of birds responds to visual motion. J Comp Physiol A. 1994; 174:297–304. [PubMed: 8151521]

Watanabe M. Synaptic organization of the nucleus dorsolateralis anterior thalami in the Japanese quail (*Coturnix coturnix japonica*). Brain Res. 1987; 401:279–291. [PubMed: 3815098]

Watts AG, Swanson LW. Efferent projections of the suprachiasmatic nucleus: II. Studies using retrograde transport of fluorescent dyes and simultaneous peptide immunohistochemistry in the rat. J Comp Neurol. 1987; 258:230–252. [PubMed: 2438309]

Watts AG, Swanson LW, Sanchez-Watts G. Efferent projections of the suprachiasmatic nucleus: I. Studies using anterograde transport of *Phaseolus vulgaris* leucoagglutinin in the rat. J Comp Neurol. 1987; 258:204–229. [PubMed: 3294923]

Wu CC, Russell RM, Karten HJ. The transport rate of cholera toxin B subunit in the retinofugal pathways of the chick. Neurosci. 1999; 92:665–676.

Wu CC, Russell RM, Nguyen RT, Karten HJ. Tracing developing pathways in the brain: a comparison of carbocyanine dyes and cholera toxin B subunit. Neurosci. 2003; 117:831–845.

Wu WQ, McGoogan JM, Cassone VM. Circadian regulation of visually evoked potentials in the domestic pigeon, *Columba livia*. J Biol Rhythms. 2000; 15:317–328. [PubMed: 10942263]

Yamazaki S, Numano R, Abe M, Hida A, Takahashi R, Ueda M, Block GD, Sakaki Y, Menaker M, Tei H. Resetting central and peripheral circadian oscillators in transgenic rats. Science. 2000; 288:682–685. [PubMed: 10784453]

Yasuo S, Watanabe M, Okabayashi N, Ebihara S, Yoshimura T. Circadian clock genes and photoperiodism: comprehensive analysis of clock gene expression in the mediobasal hypothalamus, the suprachiasmatic nucleus, and the pineal gland of Japanese Quail under various light schedules. Endocrinology. 2003; 144:3742–3748. [PubMed: 12933643]

Yoshimura T, Yasuo S, Suzuki Y, Makino E, Yokota Y, Ebihara S. Identification of the suprachiasmatic nucleus in birds. Am J Physiol. 2001; 280:R1185–1189.

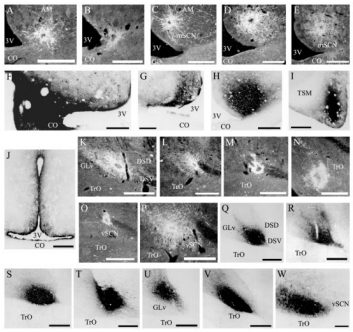

Fig. 1.

Photomicrographs documenting all biotin dextran amine (BDA) and cholera toxin B subunit (CTB) iontophoretic injections reported in Tables 2 and 3. BDA injections directed toward mSCN landed as follows: **A,B** mSCN, **C** mSCN/AM, **D** AM, **E** AM/POA. CTB injections directed at mSCN landed as follows: **F** mSCN/POA/CO, **G** mSCN/3V, **H** mSCN/AM, **I** POA, **J** 3V. BDA injections directed toward mSCN landed as follows: **K**–**M** vSCN, **N** TrO, **O** DSV, **P** dorsal to vSCN. CTB injections directed toward vSCN landed as follows: **Q**–**S** vSCN, **T** vSCN and dorsal to vSCN and WM (defined in Results), **U** ICT, **V** vSCN/GLv, **W** GLv. For abbreviations, see list. Scale bar = 1 mm in C–V; 400 μm in A,B,W.

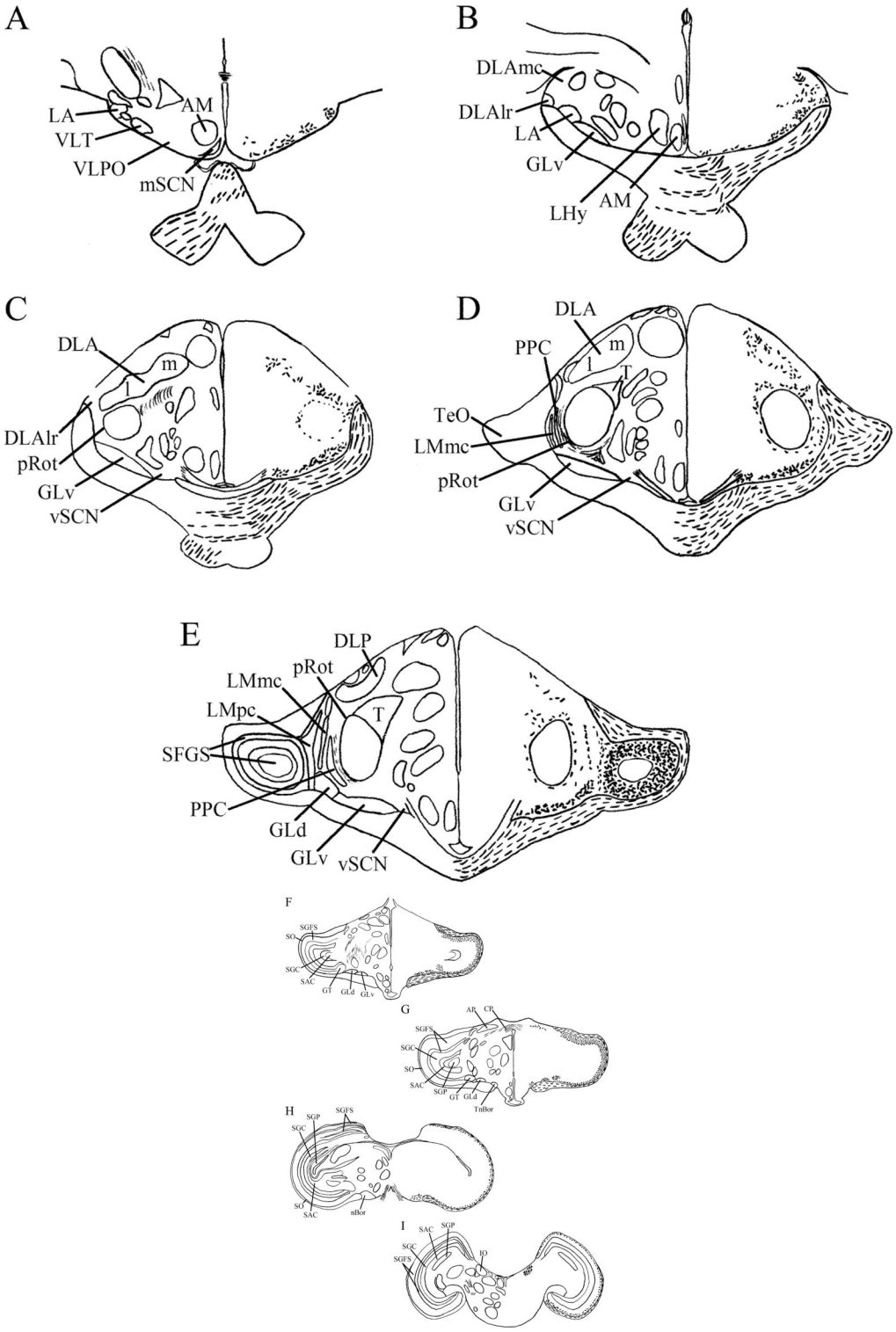

Fig. 2.

A–I: Maps of retinal input throughout its rostrocaudal extent following CTB injection to the vitreous chamber of the eye. Structures of interest are labeled on the left hemisphere of each brain and retinal fibers are indicated on the right hemispheres with short lines. **I** Cells are

indicated in IO. All fibers shown are terminal fibers. The distribution of lines represents the relative strength of input to each area, but do not represent measured values. For abbreviations, see list.

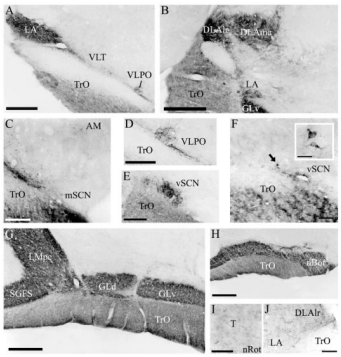

Fig. 3.

A–H: Representative photomicrographs of retinal input to the brain following CTB injection to the vitreous chamber of the eye. Note the sparse terminal fibers in the lateral mSCN after a 5-day survival period, as well as a dense grouping of fibers of passage on the lateral border (C) and the presence of cells in the anterior vSCN after two days of transport (E). For abbreviations, see list. Scale bar = 1 mm in A,B,G,H; 400 μm in E,C,D; 200 μm in I,J; 100 μm in F inset.

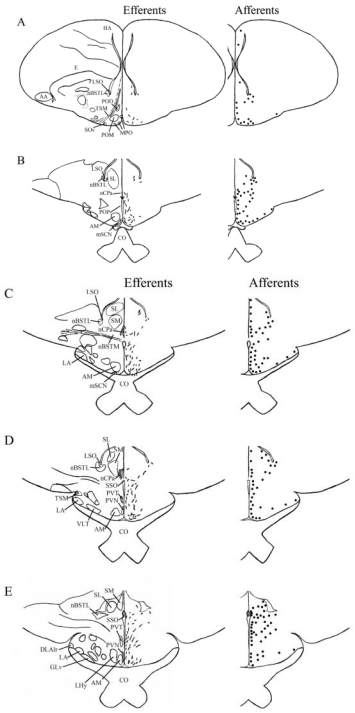

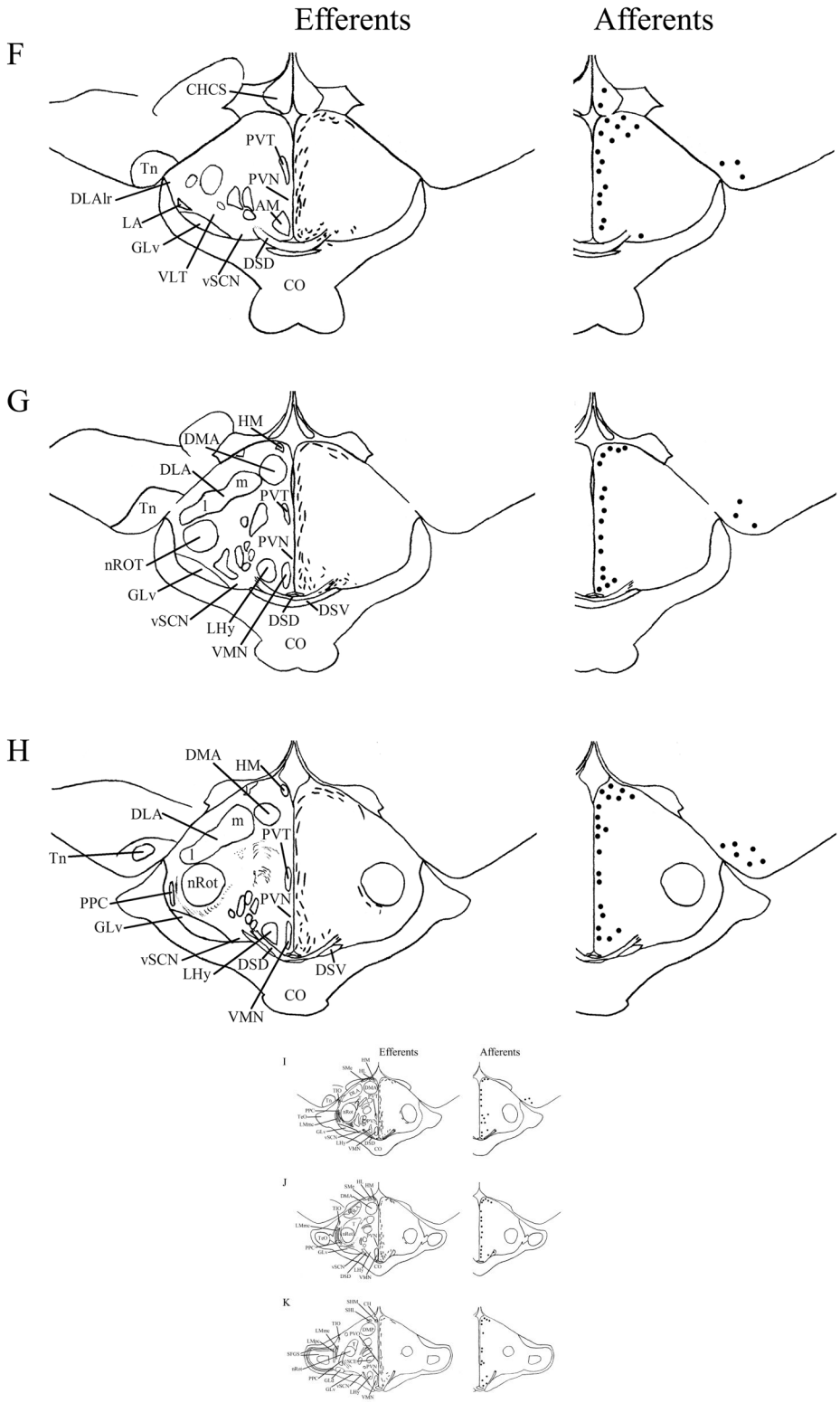

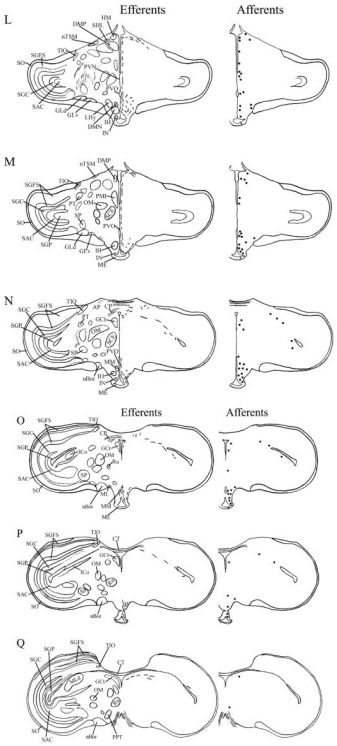

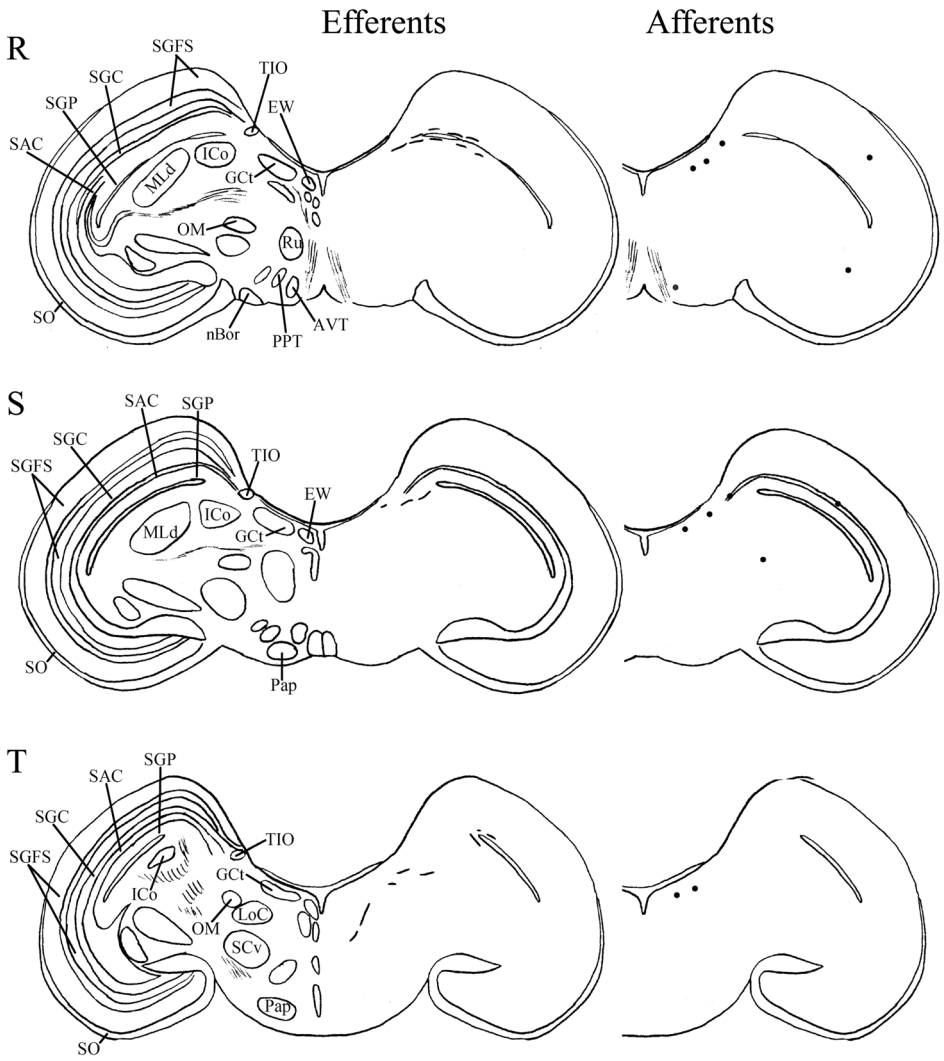

Fig. 4.

A–T: Maps of ipsilateral mSCN efferents and afferents throughout the rostrocaudal extent of the brain following BDA and CTB iontophoretic injections, respectively. Structures of interest are labeled on the left hemisphere of the brains in the left panel. Fibers in mSCN efferents are indicated on the right hemispheres of the left panel by short lines. No distinction is made between terminal fibers and fibers of passage. A summary of terminal efferents is available in Table 2. Afferents are indicated on the right panel by dark circles representing cells and are summarized in Table 3. The distribution of fibers and cells on these maps represent the relative strength of staining in these areas, but do not reflect measured values. For abbreviations, see list.

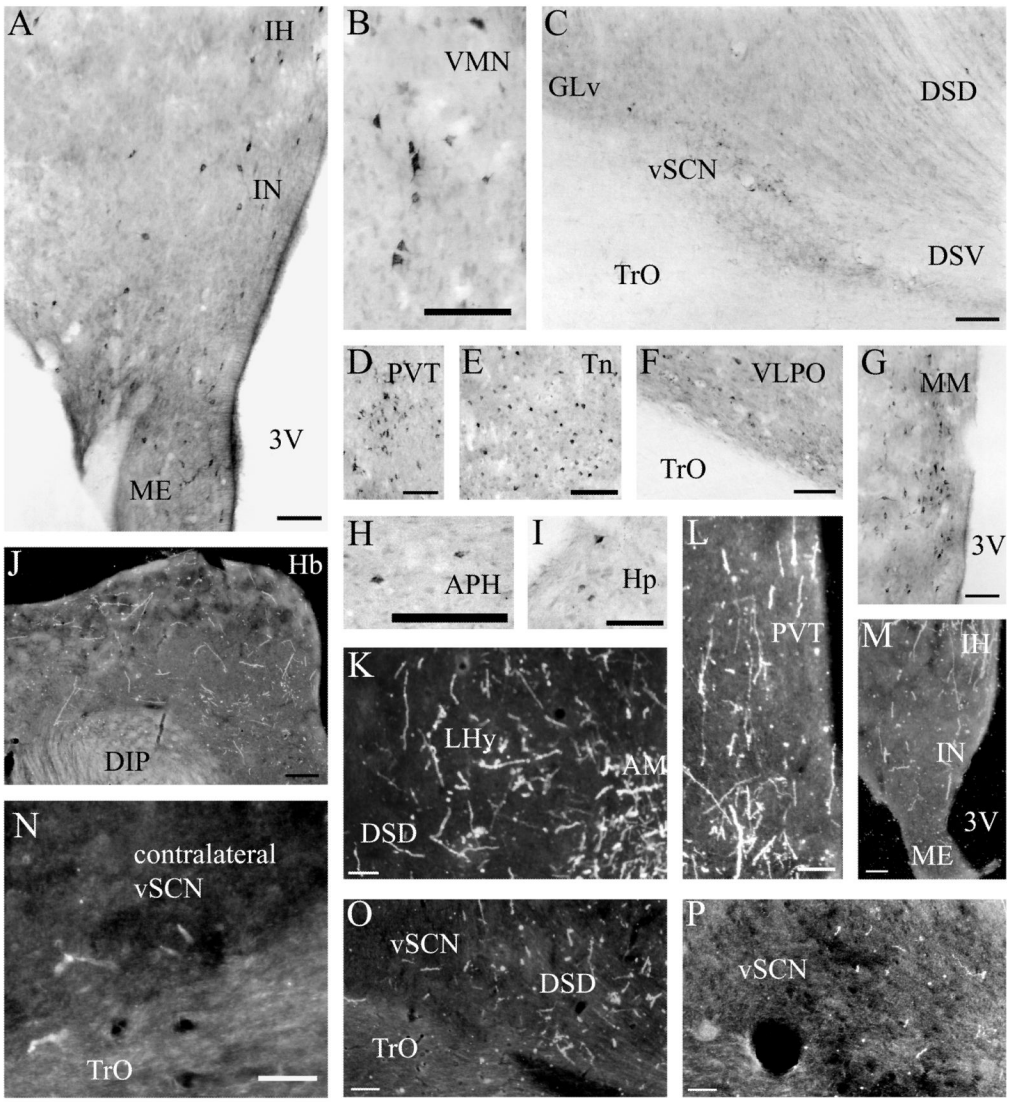

Fig. 5.

A–I: Representative photomicrographs of mSCN afferents following CTB iontophoretic injections. Note the label in the vSCN (C) and MM (G). **H–M**: Representative photomicrographs of mSCN efferents following BDA iontophoretic injections. Note the presence of terminals in both the ipsilateral (O,P) and contralateral (N) vSCN. For abbreviations, see list. Scale bar = 1 mm in J; 400 μm in A–H,K–M,O; 200 μm in I,N,P.

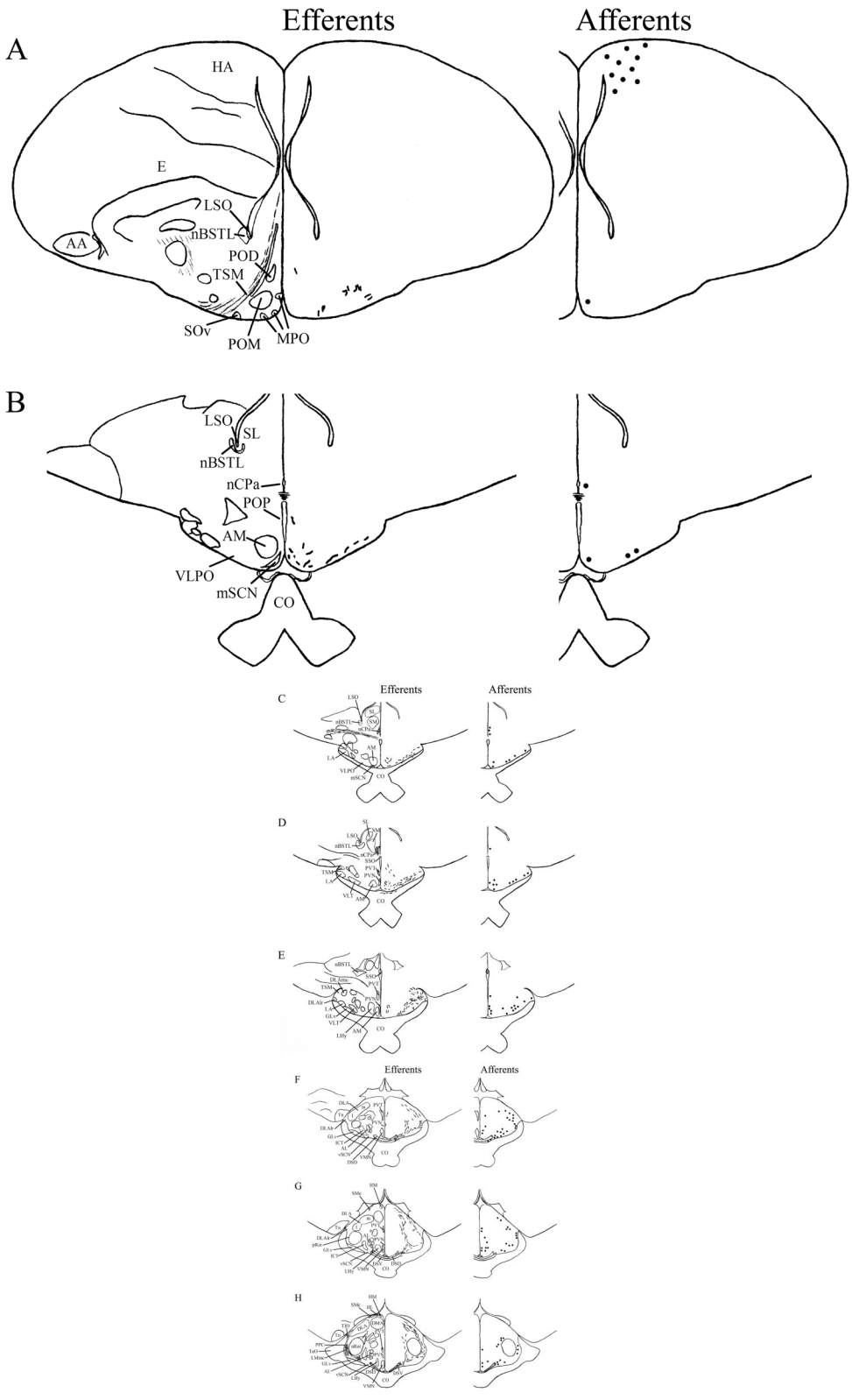

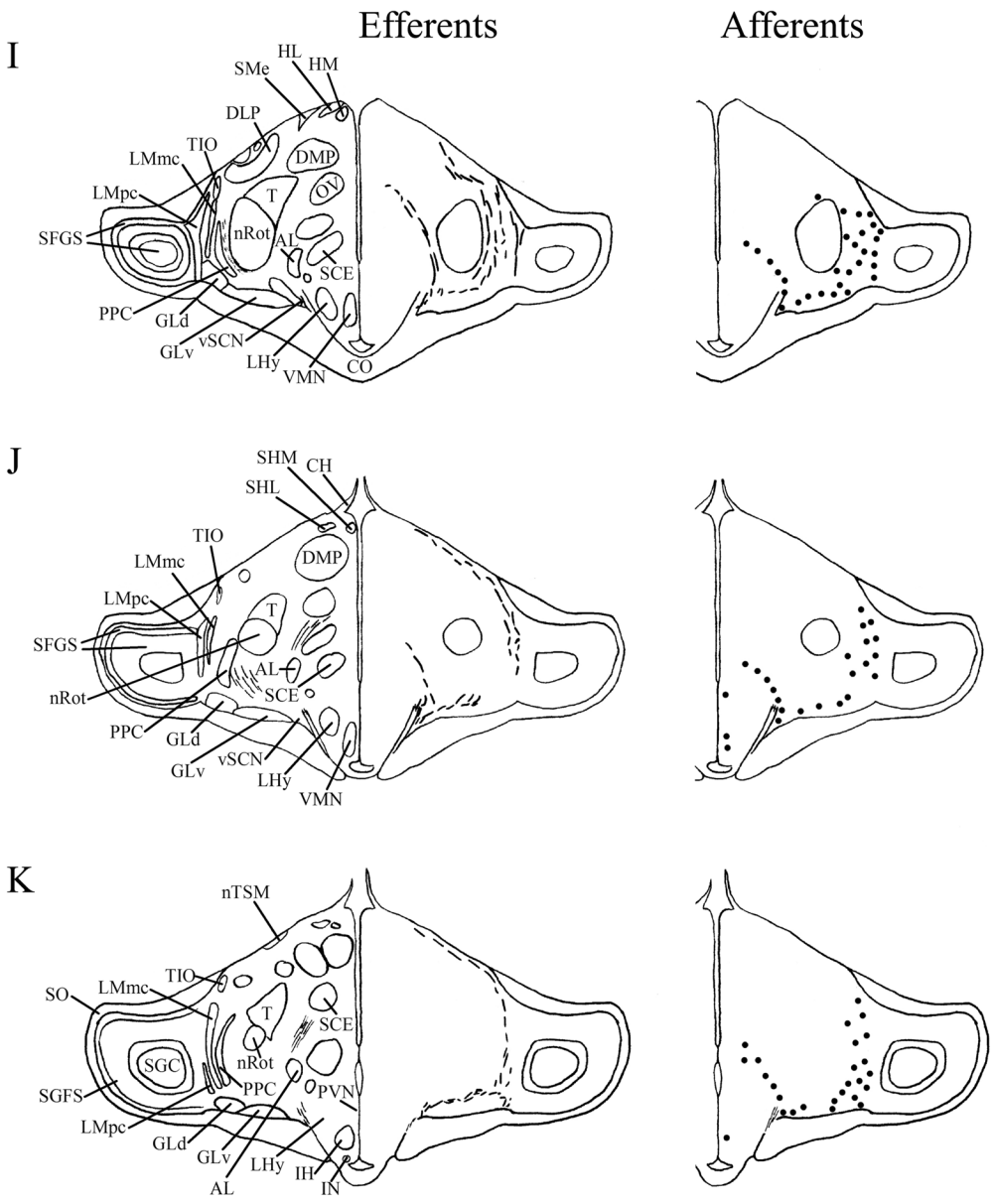

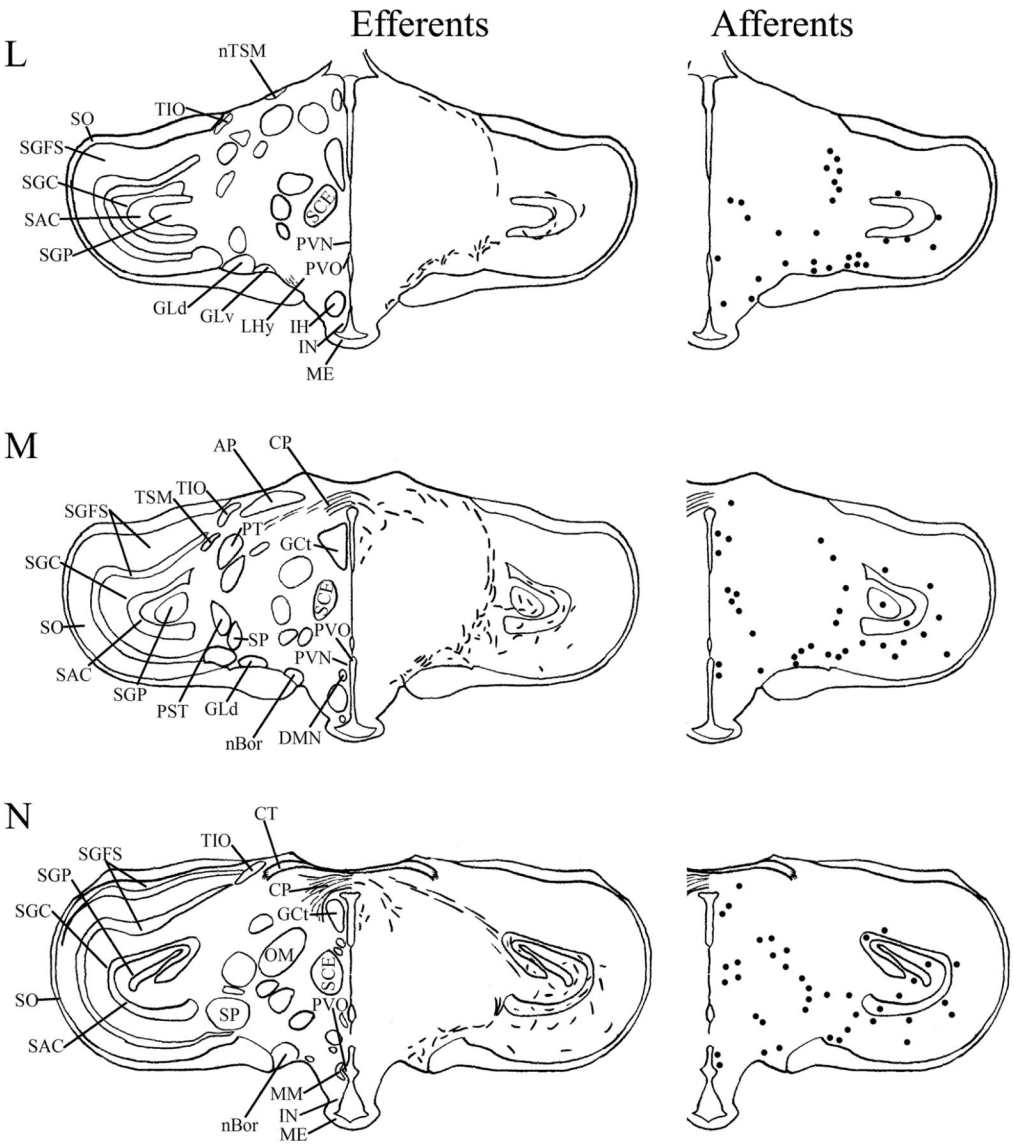

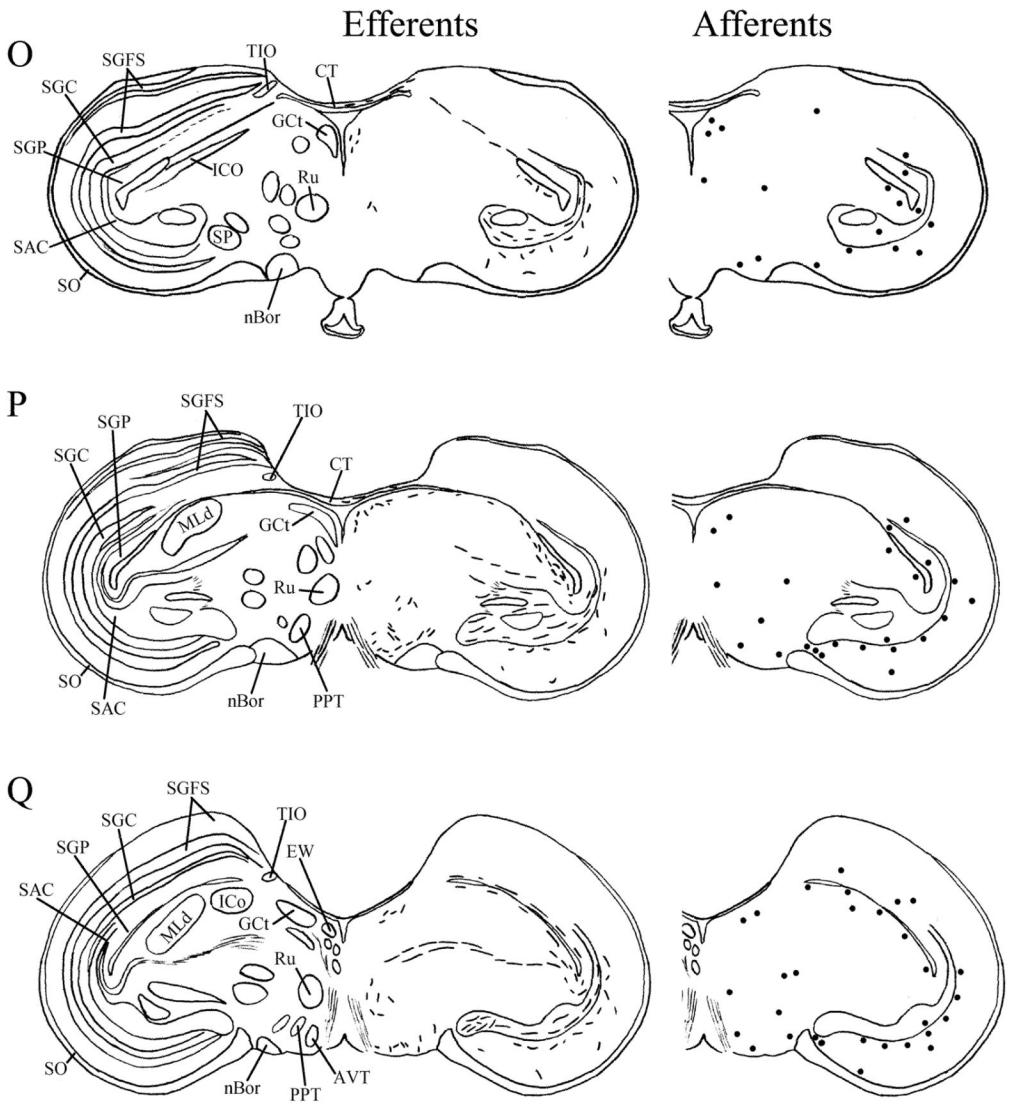

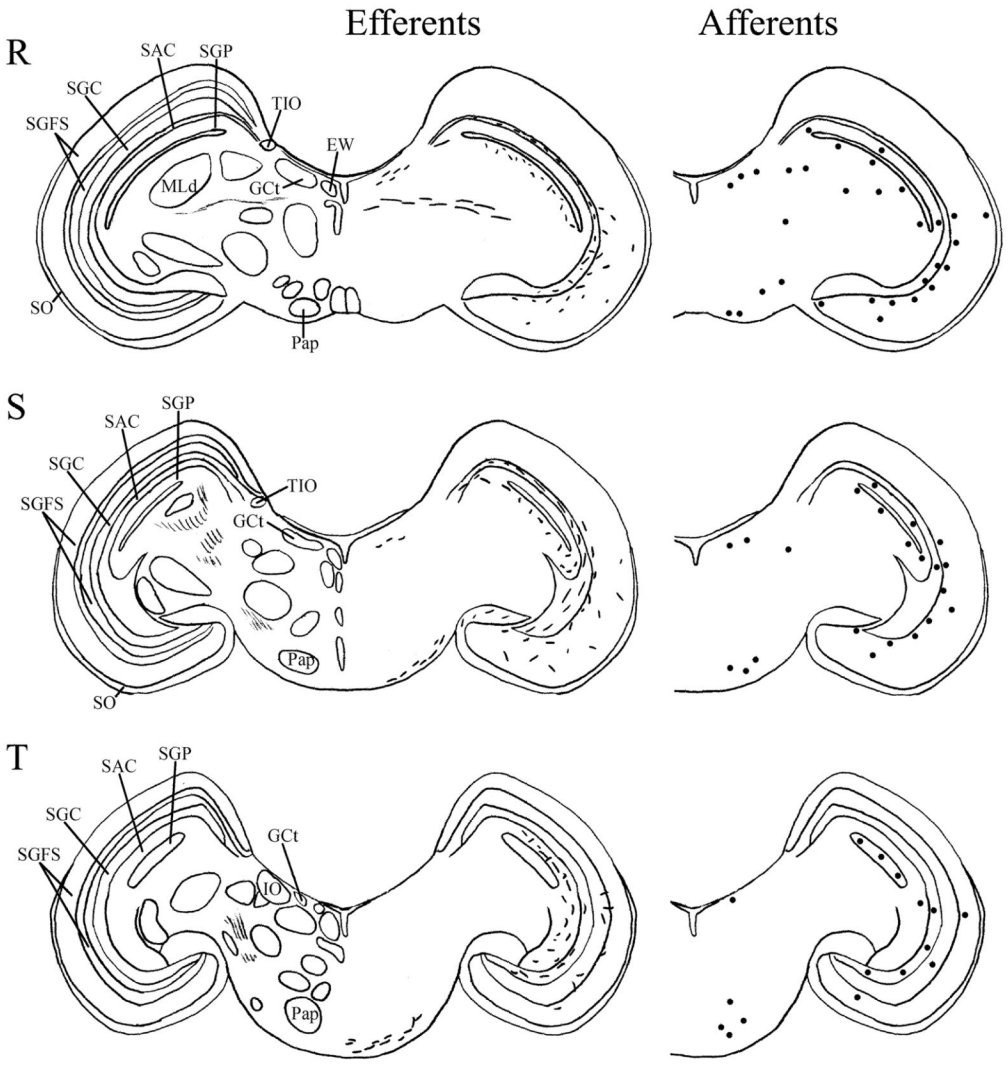

Fig. 6.

A–T: Maps of ipsilateral vSCN efferents and afferents throughout the rostrocaudal extent of the brain following BDA and CTB iontophoretic injections, respectively. Structures of interest are labeled on the left hemisphere of the brains in the left panel. Fibers in vSCN efferents are indicated on the right hemispheres of the left panel by short lines. No distinction is made between terminal fibers and fibers of passage. A summary of terminal efferents is available in Table 2. Afferents are indicated on the right panel by dark circles representing cells and are summarized in Table 3. The distribution of fibers and cells on these maps represent the relative strength of staining in these areas, but do not reflect measured values. For abbreviations, see list.

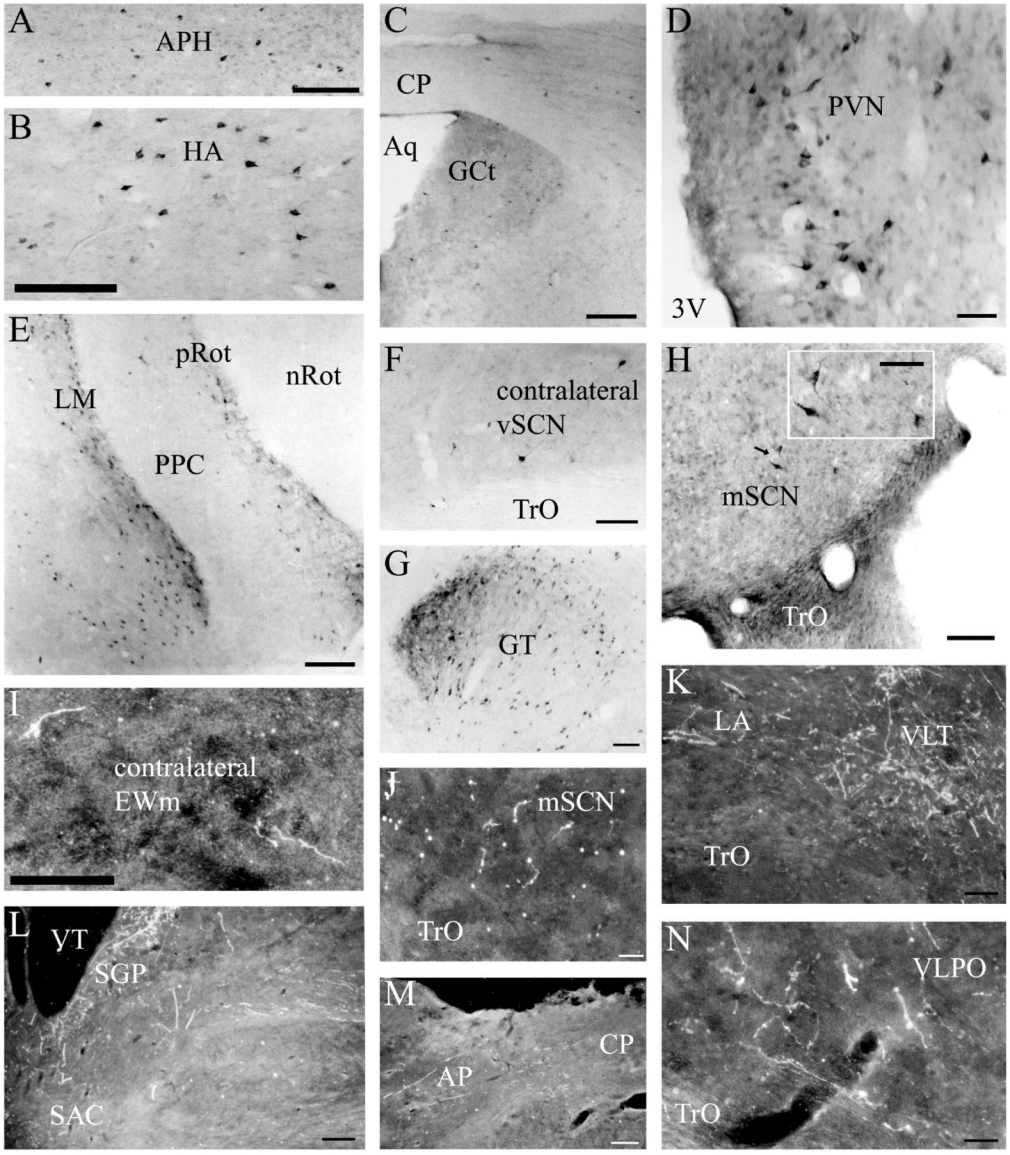

Fig. 7.

A–H: Representative photomicrographs of vSCN afferents following CTB iontophoretic injections. Note the label in the contralateral vSCN (F) and mSCN (H). **I–N**: Representative photomicrographs of vSCN efferents following BDA iontophoretic injections. Note the presence of terminals in the mSCN (J) and contralateral EWm (I). For abbreviations, see list. Scale bar = 1 mm in C,E,L,M; 400 μm in A,B,F-H,K; 200 μm in D,H inset,I,J,N.

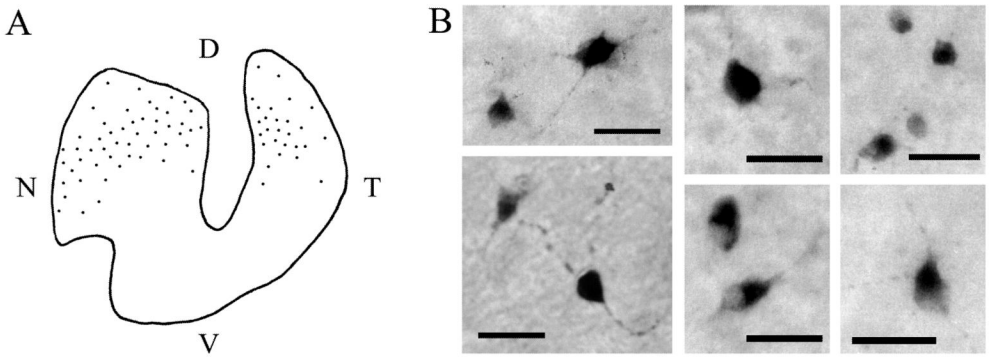

Fig. 8.

A: A distribution map of retinal ganglion cells (RGCs) involved in the retinohypothalamic tract (RHT). CTB was iontophoresed into the vSCN and allowed to trace back to the retina. RGCs projecting to the vSCN are present only in the dorsal retina. **B**: Photomicrographs of representative RGCs, which have a variety of morphologies. Chick RGCs have not been characterized by function. Scale bars in B = 100 μm.

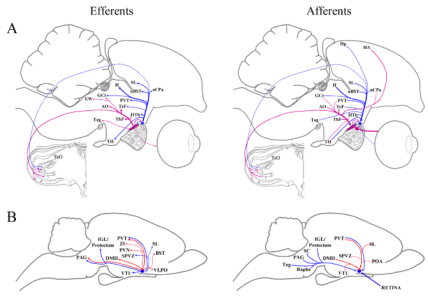

Fig. 9.

These schematic diagrams in the sagittal plane summarize what is known about the efferent and afferent connections of the chick (A) and rodents (B). The thickness of the lines represents the relative density of each projection. **A**: These drawings represent the connections of the vSCN (purple) and mSCN (blue). TeO layers: 1, SGP; 2, SAC; 3, SGC; 4, SGFS. Due to space constrictions, structures of TeF, ThF, AO and HTh were grouped together. These structures are considered individually in Tables 2 and 3. For chick structure abbreviations, see list. **B**: Summary of projections from the core (blue) and shell (red) of the mammalian suprachiasmatic nucleus (SCN). Mammalian structure abbreviations: BST, bed nucleus of the stria terminalis; DMH, dorsomedial hypothalamic nucleus; IGL, intergeniculate leaflet; PAG, periaqueductal gray; POA, preoptic area; PVN, hypothalamic paraventricular nucleus; PVT, thalamic paraventricular nucleus; SC, superior colliculus; SL, lateral septal nucleus; SPVZ, subparaventricular zone; Teg, tegmentum; VLPO, ventrolateral preoptic nucleus; VTU, ventral tuberal hypothalamus; ZI, zona incerta.

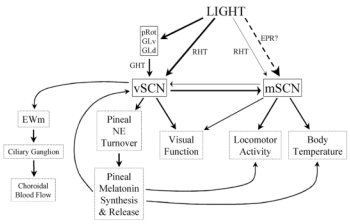

Fig. 10.

A working model of the avian SCN. This model addresses the transduction of light to the SCN and summarizes what we hypothesize are the roles of the vSCN and mSCN in the circadian system. Solid lines represent connections reported in the current study and the literature. The dashed line represents speculation based on indirect evidence. For abbreviations, see list.